SYNTHESIS OF A POTENTIAL REDOX ACTIVE LIGAND FOR PLATINUM COMPLEXES

by

Didem Erkut

B.S., Integrated Bs and Ms Program in Chemistry Education, Boğaziçi University, 2013

Submitted to the Institute for Graduate Studies in
Science and Engineering in partial fulfillment of
the requirements for the degree of
Master of Science

Graduate Program in Chemistry
Bogazici University
2018

SYNTHESIS OF A POTENTIAL REDOX ACTIVE LIGAND FOR PLATINUM COMPLEXES

APPROVED BY:

Assoc. Prof. A. Ersin Acar …….
(Thesis Supervisor)

Assoc. Prof. Ece Bulak …….

Prof. Dr. Safiye Erdem …….

DATE OF APPROVAL: 23.05.2018

Dedicated to My Family and Altemur

ACKNOWLEDGEMENTS

At the beginning, I would like to extend my sincere gratitude to my supervisor Assoc. Prof. Ali Ersin Acar for accepting me his research group. I am thankful to him for his guidance, encouragement, support and patience. I learned a lot from him not only about chemistry but also about life.

I would like to thank to Assoc. Prof. Ece Bulak for her support and giving me the chance to work in her laboratory and the project. I would like to thank my committee member Prof. Dr. Safiye Erdem for giving her valuable time for reviewing my thesis.

During my thesis I worked with wonderful research group whose people always give me big support. Firstly, I would like to thank to Ayşenur for her unrequited help and support at any time. My appreciations go to Işıl, Kamil, Halenur, Sedef, Seda, Duygu, Aylin and Ahmet. They willingly helped me out with their abilities. Without our smiles, experiences about life and chemistry, I could not be as happy as in the laboratory and my life. I would like to express my gratitude to all people I work with "Acar Lab" for their help and friendship.

In addition, very special thanks to my dearest friends Merve, Melike and Gizem for their encouragement, friendship and all the memories.

This thesis would not have been possible without my family. I would like to especially thank to my aunt Nergül and uncle Salim for their support throughout my life.

Finally, I would like to acknowledge with gratitude the support, encouragement, belief and love of my parents; Hacer and Ferhat Erkut. I owe them a lot. Without them I couldn't be able to the person who I am. My sister İrem is always my best friend and my biggest support. I could not imagine a life or a moment without her.

Lastly, I would like to thank to Altemur. I am always grateful having him in my life for being behind me under any circumstances, at any time, supporting me and making me happy. He always gives me the motivation for my work and the most value to my life.

ABSTRACT

SYNTHESIS OF A POTENTIAL REDOX ACTIVE LIGAND FOR PLATINUM COMPLEXES

Redox active ligands can cooperate with the metal in a synergistic manner and their interplay facilitates the chemical process especially in the catalytic reactions. In this research, the ligand part has a quinoxaline structure. Quinoxaline compounds are essential nitrogen containing heterocyclic compounds of various biological properties (i.e. anti-tumor, anti-cancer) thus they have several pharmaceutical applications. It is also known that quinoxaline derivatives have a very wide range of applications in electrical and photochemical agents as well. The ligand has an extended π conjugated system, properties such as photoluminescence and fluorescence are expected to be observed. The yield optimization of two different functionalized quinoxalines as potential redox active ligands with air free conditions and syntheses of their platinum complexes were studied in this research. The goal of this study is to synthesize a platinum complex with redox active ligand. Coordination was observed from thermal, ^{1}H NMR and fluorescence spectroscopic analyses for both of the complexes. Physical and chemical characterization of the synthesized ligands and complexes were determined *via* ^{1}H and ^{13}C NMR, DSC, fluorescent and UV-Vis spectrophotometer. It was shown that both of these ligands can act as ligands to transition metals the first example was with platinum.

ÖZET

PLATİN KOMPLEKSLERİ İÇİN POTANSİYEL REDOKS AKTİF LİGAND SENTEZİ

Redoks aktif ligandlar, metal ile sinerjik bir şekilde işbirliği yapabilir ve etkileşimleri, özellikle katalitik reaksiyonlarda kimyasal işlemi kolaylaştırır. Bu araştırmada, ligand kısmı bir kinoksal yapıya sahiptir. Kinoksalin bileşikleri, çeşitli biyolojik özelliklere (anti-tümör, anti-kanser gibi) sahip olan Nitrojen içeren heterosiklik bileşiklerdir ve bu nedenle farmasötik uygulamaya sahiptirler. Ayrıca, kinoksalin türevlerinin, elektrik ve fotokimyasal ajanlarda da çok geniş bir uygulama alanına sahip olduğu bilinmektedir. Ligand genişletilmiş π konjuge sistemine sahiptir, fotolüminesans ve flüoresan gibi özelliklerin gözlenmesi beklenmektedir. Bu çalışmada, iki farklı işlevselleştirilmiş kinoksalin, serbest redoks aktif ligandlar ve Platin komplekslerinin sentezleri ile verim optimizasyonu incelenmiştir. Bu çalışmanın amacı redoks aktif ligand ile bir Platin kompleksinin sentezlenmesidir. Her iki kompleks için de termal, ^{1}H NMR ve floresan spektroskopik analizlerden koordinasyon gözlenmiştir. Sentezlenen ligandların ve komplekslerin fiziksel ve kimyasal karakterizasyonu, ^{1}H ve ^{13}C NMR, DSC, floresan ve UV-Vis spektrofotometre ile belirlenmiştir. Bu ligandların her ikisinin de geçiş metallerine ligand olarak davranabileceği gösterilmiştir ve ilk örnek Platin'dur.

TABLE OF CONTENTS

ACKNOWLEDGEMENTS IV

ABSTRACT V

ÖZET VI

TABLE OF CONTENTS VII

LIST OF FIGURES X

LIST OF TABLES XIII

LIST OF ACRONYMS/ABBREVIATIONS XIV

1. INTRODUCTION 1

    1.1. Quinoxalines 1

    1.2. Electronic and Electroluminescent Properties of Quinoxalines 2

    1.3. Redox Active Ligands 3

    1.4. Metal Complexes with Non-innocent Ligands 5

    1.5. Metal Complexes of Quinoxaline Ligands 6

    1.6. Platinum Complexes 6

    1.7. Synthetic Routes to Quinoxaline Structure 8

2. AIM OF THE STUDY 9

3. EXPERIMENTAL 10

    3.1. Methods and Materials 10

    3.2. Instrumentation 10

3.3. Synthesis of the Ligands 11
3.3.1. Synthesis of Acenaphtho [1,2-b] quinoxaline-9, 10-diamine 11
3.3.2. Synthesis of Acenaphtho [1, 2-b] quinoxaline-9, 10-diamine dihydrochloride 12
3.3.3. Synthesis of N^9, N^9, N^{10}, N^{10}-tetramethylacenaphtho [1, 2-b] quinoxaline-9, 10-diamine 13

3.4. Synthesis of the Complexes 14
3.4.1. Synthesis of Acenaphtho [1, 2-b] quinoxaline-9, 10-diamine Platinum Complex 14
3.4.2. Synthesis of N^9, N^9, N^{10}, N^{10}-tetramethylacenaphtho [1, 2-b] quinoxaline-9, 10-diamine Platinum Complex 14

4. RESULTS AND DISCUSSION 16

4.1. Syntheses of Acenaphtho [1, 2-b] quinoxaline-9, 10-diamine and Acenaphtho [1, 2-b] quinoxaline-9, 10-diamine dihydrochloride 16

4.2. Synthesis of N^9, N^9, N^{10}, N^{10}-tetramethylacenaphtho [1, 2-b] quinoxaline-9, 10-diamine 17

4.3. Synthesis of Acenaphtho [1, 2-b] quinoxaline-9, 10-diamine Platinum Complex 18

4.4. Synthesis of N^9, N^9, N^{10}, N^{10}-tetramethylacenaphtho [1, 2-b] quinoxaline-9, 10-diamine Platinum Complex 20

4.5. UV - Vis Spectra of Synthesized Molecules 20

4.6. Fluorescence Spectra of Synthesized Molecules 23

4.7. Cyclic Voltammetry Analysis of the Synthesized Molecules 26

4.8. Thermal Analysis of Synthesized Molecules 28

5. CONCLUSIONS 33

6. FUTURE WORK 34

REFERENCES 35

APPENDIX A: SPECTROSCOPY DATA 41

LIST OF FIGURES

Figure 1.1. The fusion of benzene and pyrazine to form quinoxaline structure [2]. 1

Figure 1.2. Redox active (electrochemically active) ligands [20]. 3

Figure 1.3. General representation of four main strategies of using redox non-innocent ligands in catalysis [17]. 4

Figure 1.4. Synthetic Approach for Quinoxalinones 1, 1,2,3,4-Tetrahydroquinoxalines 2, Quinoxalines 3, and Quinoxalin-2(1H)-ones 4 [45]. 8

Figure 3.1. Synthesis of Acenaphtho [1, 2-b] quinoxaline-9, 10-diamine. 11

Figure 3.2. Synthesis of Acenaphtho [1, 2-b] quinoxaline-9, 10-diamine dihydrochloride. 12

Figure 3.3. Synthesis of N9, N9, N10, N10-tetramethylacenaphtho [1, 2-b] quinoxaline-9, 10-diamine. 13

Figure 3.4. Synthesis of Acenaphtho [1, 2-b] quinoxaline-9, 10-diamine Platinum Complex. 14

Figure 3.5. Synthesis of N^9, N^9, N^{10}, N^{10}-tetramethylacenaphtho [1, 2-b] quinoxaline-9, 10-diamine Platinum Complex. 15

Figure 4.1. Mechanism of Acenaphtho [1, 2-b] quinoxaline-9, 10-diamine Reaction. . 17

Figure 4.2. Mechanism of N9, N9, N10, N10- tetramethylacenaphtho [1, 2-b] quinoxaline-9, 10-diamine Reaction. 18

Figure 4.3. Acenaphtho [1, 2-b] quinoxaline-9, 10-diamine Platinum complex structure. 19

Figure 4.4. UV – Vis Spectrum of acenaphtho [1, 2-b] quinoxaline-9, 10-diamine. 20

Figure 4.5. UV – Vis Spectrum of acenaphtho [1, 2-b] quinoxaline-9, 10-diamine dihydrochloride. 21

Figure 4.6. UV – Vis Spectrum of acenaphtho [1, 2-b] quinoxaline-9, 10-diamine Platinum Complex. 21

Figure 4.7. UV – Vis Spectrum of N^9, N^9, N^{10}, N^{10}- tetramethylacenaphtho [1, 2-b] quinoxaline-9, 10-diamine. 22

Figure 4.8. UV – Vis Spectrum of N^9, N^9, N^{10}, N^{10}- tetramethylacenaphtho [1, 2-b] quinoxaline-9, 10-diamine Platinum Complex. 23

Figure 4.9. Fluorescence Spectrum of acenaphtho [1, 2-b] quinoxaline-9, 10-diamine (activation λ = 442 nm). 23

Figure 4.10. Fluorescence Spectrum of acenaphtho [1, 2-b] quinoxaline-9, 10-diamine dihydrochloride (activation λ = 438 nm). 24

Figure 4.11. Fluorescence Spectrum of acenaphtho [1, 2-b] quinoxaline-9, 10-diamine Platinum Complex (activation λ = 354 nm). 24

Figure 4.12. Fluorescence Spectrum of N^9, N^9, N^{10}, N^{10}- tetramethylacenaphtho [1, 2-b] quinoxaline-9, 10-diamine (activation λ = 439 nm). 25

Figure 4.13. Fluorescence Spectrum of N^9, N^9, N^{10}, N^{10}- tetramethylacenaphtho [1, 2-b] quinoxaline-9, 10-diamine Platinum Complex (activation λ = 432 nm). ... 25

Figure 4.14. Cyclic Voltammogram of Acenaphtho [1, 2-b] quinoxaline-9, 10-diamine.26

Figure 4.15. Cyclic Voltammogram of Acenaphtho [1, 2-b] quinoxaline-9, 10-diamine dihydrochloride. 27

Figure 4.16. DSC Spectrum of acenaphtho [1, 2-b] quinoxaline-9, 10-diamine. 28

Figure 4.17. DSC Spectrum of acenaphtho [1, 2-b] quinoxaline-9, 10-diamine dihydrochloride. 28

Figure 4.18. DSC Spectrum of acenaphtho [1, 2-b] quinoxaline-9, 10-diamine Platinum Complex. 29

Figure 4.19. DSC Spectrum of N^9, N^9, N^{10}, N^{10}- tetramethylacenaphtho [1, 2-b] quinoxaline-9, 10-diamine. 29

Figure 4.20. Spectrum of N^9, N^9, N^{10}, N^{10}- tetramethylacenaphtho [1, 2-b] quinoxaline-9, 10-diamine platinum complex. 30

Figure 4.21. DSC Spectrum of $PtCl_2(DMSO)_2$. 30

Figure A.1. ^{1}H-NMR Spectrum of Acenaphtho [1, 2-b] quinoxaline-9, 10-diamine in $(CD_3)_2CO$. 42

Figure A.2. ^{13}C-NMR Spectrum of Acenaphtho [1, 2-b] quinoxaline-9, 10-diamine in d_8THF. 43

Figure A.3. ^{1}H-NMR Spectrum of Acenaphtho [1, 2-b] quinoxaline-9, 10-diamine dihydrochloride in d_8THF. 44

Figure A.4. ^{13}C-NMR Spectrum of Acenaphtho [1, 2-b] quinoxaline-9, 10-diamine dihydrochloride in d_8THF. 45

Figure A.5. ^{1}H-NMR Spectrum of N^9, N^9, N^{10}, N^{10}- tetramethylacenaphtho [1, 2-b] quinoxaline-9, 10-diamine in $CDCl_3$. 46

Figure A.6. ^{13}C-NMR Spectrum of N^9, N^9, N^{10}, N^{10}- tetramethylacenaphtho [1, 2-b] quinoxaline-9, 10-diamine in $CDCl_3$. 47

Figure A.7. ^{1}H-NMR Spectrum of Acenaphtho [1, 2-b] quinoxaline-9, 10-diamine in CD_3CN. 48

Figure A.8. ^{1}H-NMR Spectrum of Acenaphtho [1, 2-b] quinoxaline-9, 10-diamine Platinum Complex in CD_3CN. 49

LIST OF TABLES

Table 4.1.Melting Points of the Synthesized Compounds according to DSC Results 31

LIST OF ACRONYMS/ABBREVIATIONS

Ag	Silver
AgCl	Silver chloride
Bu_4NPF_6	Tetrabutylammonium hexafluorophosphate
CD_3Cl	Deuterated chloroform
CD_3CN	Deuterated acetonitrile
DMSO	Dimethyl sulfoxide
DNA	Deoxyribonucleic acid
DPQ	2,3-bis(2-pyridyl)- quinoxaline
DSC	Differential scanning calorimetry
d_8THF	Deuterated tetrahydrofuran
EtOAc	Ethyl acetate
EtOH	Ethanol
H	Hydrogen
H_2O	Water
LUMO	Lowest Unoccupied Molecular Orbital
N	Nitrogen
$NaHCO_3$	Sodium bicarbonate

Na_2SO_4	Sodium sulfate
NMR	Nuclear Magnetic Resonance
OLED	Organic light-emitting devices
Pt	Platinum
$Pt(DMSO)_2Cl_2$	cis-Dichlorobis(dimethyl sulfoxide)platinum(II)
UV	Ultraviolet

1. INTRODUCTION

1.1. Quinoxalines

Quinoxalines are made up of two aromatic rings; benzene and pyrazine, therefore, they are also called benzopyrazine (Figure 1.1.). Quinoxaline is one of the most common heterocyclic scaffolds used. They are also used as bioisosters of quinolines, naphthalenes and benzothiophenes [1].

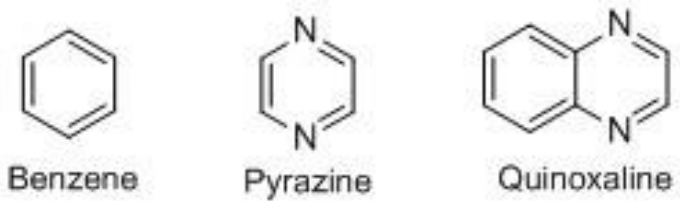


Figure 1.1. The fusion of benzene and pyrazine to form quinoxaline structure [2].

Quinoxaline and its derivatives are integral part of pharmacologically active molecules, they exhibit antithrombotic, antiviral, antidepressant, antimalarial, anticonvulsant, antituberculosis, antibacterial, anticancer, anti HIV, anti-inflammatory, antifungal, antineoplastic, antiglucoma, antimicrobial properties [3].

Transition-metal quinoxaline complexes have been under investigation for their anticancer properties such as 2,3-bis(2-pyridyl)- quinoxaline (DPQ) which was shown to bind to DNA. In addition, some quinoxaline-2,3-diones and quinoxalin-2-ones show novel, anti-pain, antimicrobial, anti-inflammatory and potent antithrombotic activities [2].

1.2. Electronic and Electroluminescent Properties of Quinoxalines

Stability, molecular packing, solubility and electronic properties of the arenes can be tuned by changing the position and the number of incorporated amines. Moreover, addition of a five-membered ring in the arene skeleton can decrease the LUMO energy of the molecule because of the trend to accept electrons over 4n + 2 stabilization. Quinoxalines can be good chelating ligands when some functional donor groups are introduced to their structure [4].

Some metal chelating ligand substituents such as dipyrrole, crown-ether rings, and terpyridine can control electronic properties of the fluorephores. Their application to chemosensors are possible when the fluorescent optical switch occurs thanks to fluorophores. In the case of quinoxaline, it can absorb or emit wavelength through oxidation by means of nitrogen on the structure [5, 6].

Quinoxalines are characteristic fluorophores. Heterocyclic fluorophores are effective building blocks in the synthesis of biologically active molecules [7]. For this reason, potential applications such as emitters in electroluminescent devices and biochemical molecular probes are being explored [8].

Quinoxalines are also important compounds that can be used in the electroluminescent materials thanks to their structure which show similarities with natural chromophores [9]. In industrial applications, they are useful to prevent metal corrosion for preparation of porphyrins [10–12]. They have also application areas as cavitands, dyes, organic semiconductors, DNA cleaving agents and chemically controllable switches. When quinoxalines have electron withdrawing groups on their structures, they are used in π-conjugated scaffolds as a building material for the OLEDs [13].

1.3. Redox Active Ligands

The redox-active ligands are important in coordination and organometallic chemistry, especially in the area of catalysis. They can enhance the reactivity of a metal complex by steric and electronic effects. They can stabilize multi-oxidation states of a metal in a complex. They are known as redox-active and cooperative ligands (Figure 1.2.). They are involved in bond making and breaking processes, redox reactions and H-bonding interactions directly and actively during catalysis [14].

The properties of a complex come from the interaction between the ligand and the metal center, hence the properties of the complexes are determined by the ligand and metal center together. Their interplay facilitates the catalytic process. The steric and electronic features of the ligand affect the properties of the metal complex. The reactive redox active ligands have a key role in a catalytic cycle for fundamental bond activation steps. Synthesizing organic materials for the growing society is a necessity. Hence, the new catalysts which work more selectively and efficiently are needed. In that point, redox non-innocent ligands are of current interest [15–17].

These type of metal complexes are used in catalytic oxidation and reduction reactions [18]. Oxidation or reduction reaction takes place at the metal center where the ligand part is expected to stay unaffected. However, if the complex has a redox active ligand, the ligand part is also involved in the redox reaction [19].

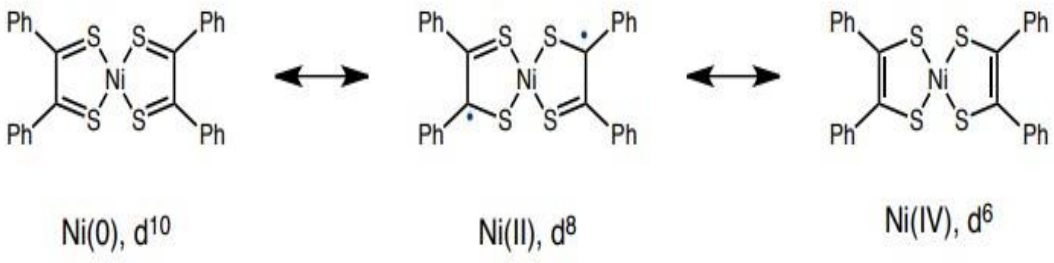


Figure 1.2. Redox active (electrochemically active) ligands [20].

The term non-innocent is used to underline the chemical involvement of the redox active ligands. Non-innocent term was used for the first time to explain oxidation state ambiguity of redox active ligands by Jørgensen [21]. His definition for innocent ligand is "Ligands are innocent when they allow oxidation states of the central atoms to be defined" [21]. Hence, non-innocent means an ambi-valence of oxidation state assignments. If ligands behave unexpectedly when they are exposed to external stimulus, this type of ligands are called as non-innocent or redox active ligands [22].

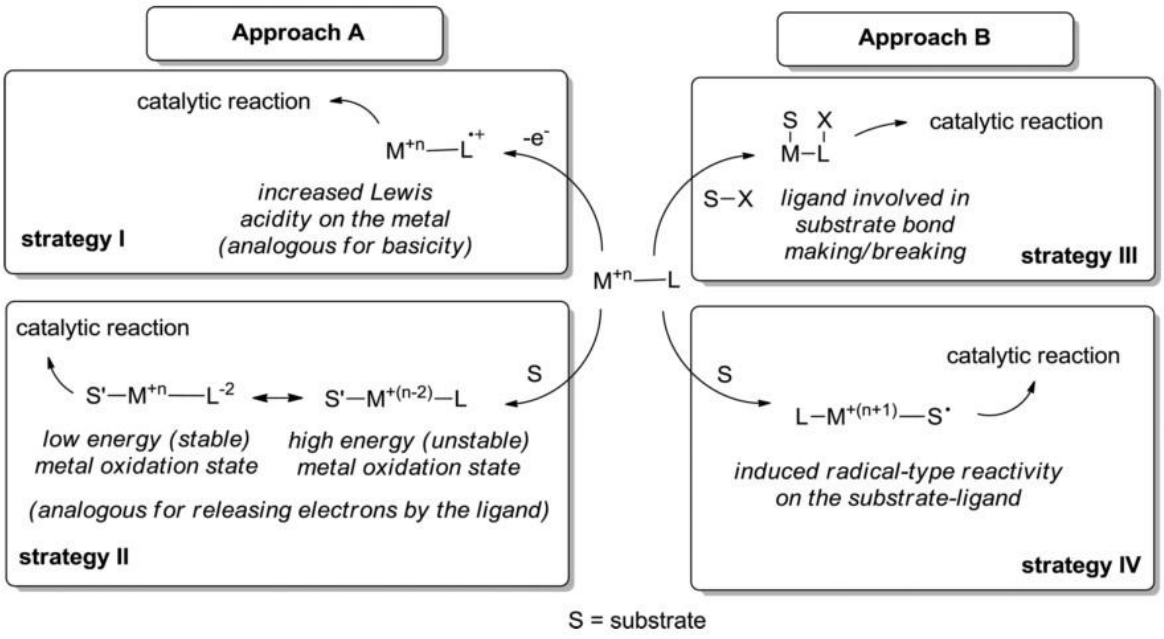


Figure 1.3. General representation of four main strategies of using redox non-innocent ligands in catalysis [17].

There are two main ways in defining the reactivity of redox active ligands (Figure 1.3.). In the first the ligands are involved in catalytic cycle by electron accepting or donating. In the second, the ligands participate to the catalytic cycle by forming or breaking covalent bonds. There are four main mechanisms involved in these reactions. In the first mechanism, the ligand changes the electronic properties of the metal center such as the Lewis acidity or basicity by oxidation and reduction. In the second one, ligand behaves as an electron reservoir which ensures the ability of the complex to make one more electron transfer. Under

normal circumstances, the complex is not willing to do more than one electron transfer. Metals usually do not adopt easily to the conditions of the high energy oxidation state. Especially first row transition metals react in a way that only one electron transfer at a time is possible. However, it is possible to have more than one electron transfer by using electron reservoir type of ligands. When there is a multi-electron transformation, ligand that is attached to metal can take additional electrons. For this reason metal center can stay in its most stable oxidation state. Oxidative additions or reductive eliminations are good examples of two-electron transfer reactions that are made possible by electron reservoir type ligands. In the third mechanism, the ligand radicals are actively involved in the reaction mechanism during the catalytic cycle. Both the redox active ligand and metal provide the activation of the substrate. They lead to the reactions which are problematic in other ways. In the last mechanism, substrate behaves like a redox active ligand and undergoes a radical type activation. The idea is that electron transfer to or from a redox active substrate imposes intrinsic radical-type behavior which often leads to typical radical-type reactivity useful in subsequent elementary steps in a catalytic cycle [17].

1.4. Metal Complexes with Non-innocent Ligands

In the coordination chemistry, metal complexes with non-innocent ligands have been known since square-planar nickel dithiolene (enedithiol) compounds were synthesized in 1960s [23]. Although the properties of the complexes are determined with non-innocent ligand and metal center together, the word “non-innocent” is only used for the ligand part [21]. However, addition of a metal to a non-innocent ligand alters the ligand reactivity. Oxidation and reduction processes are good examples of this alteration. While non-innocent ligands can be oxidized and reduced reversibly in the complex form, this transformation occurs irreversibly in the ligand itself. So, the most important feature of complexes with non-innocent ligands is that both the ligand and metal parts are involved together in many chemical and physical processes [24].

1.5. Metal Complexes of Quinoxaline Ligands

In a metal complex, the metal ion acts as an acceptor and coordinates with the ligands having at least one donor atom. If the ligand part has more than one donor atom, it forms a heterocyclic ring called a chelate ring. In that case, the ligand part can be named as chelating agent and the complex as a metal chelate [25]. Quinoxalines behave as chelating agents when they are functionalized.

Aromatic and nitrogen containing heterocycles have low π^* orbitals. These low π^* orbitals are good acceptors for the metal *d*-orbitals and suitable for back bonding. This is also valid for quinoxaline structure. Moreover, hetero atom in the ring ion radical and extended π-conjugation decrease columbic repulsion for complexation in the quinoxaline case [26].

Quinoxaline and its derivatives are bridging ligands in the case of homobimetallic and heterobimetallic complexes. Quinoxalines act as rigid sub units in macrocyclic receptors. As a consequence of their chemical and biological features, new quinoxaline derivative complexes have been of current interest. Additionally, quinoxalines are extensively found in nature. Quinoxaline derivatives are used in photovoltaics, optoelectronic devices, flame resistant polymers and they have biological applications such as the antibiotics, levomycin and actinomycin. They can be used as fluorophores, photosensitizer, corrosion inhibitor, and electron-transport material [27].

1.6. Platinum Complexes

Platinum(II) complexes are of current interest in view of their different properties. Their application is possible for the therapy of tumors [23, 24], C-H activating catalysts [30] and supporting materials in solar energy area [31]. They emit light in the solution and in solid state [32]. Physically, they can show solvatochromism, thermochromism,

vapochromism, ionochromism [33]. When platinum coordinate to a non-innocent ligand, they can be electrochemically active [34]. Their crystallization variations show disparate physical characteristics thanks to different aggregations *via* s/s or p/p interactions like stacking [35]. Also, they can be used as structure maintaining vertices in large supramolecular cores [36, 37].

Cisplatin is the most common oncological agent against various cancers such as testicles, ovaries, bladder, head and neck cancers. The discovery of *cis*-diaminedichloroplatinum(II) (*cis*-platin) and its anticancer activity as a coordination compound is one of the most important developments in the area of medicinal inorganic chemistry. However, its clinical usage is restricted by its side effects such as nephrotoxicity, ototoxicity, neurotoxicity and the emergence of drug resistance. Hence, plenty of platinum complexes have been synthesized to overcome these side effects and increase its effectiveness. However, there are main rules which were set by Cleare and Hoeschele which define the use of a platinum complex as an oncological agent [38]. First of all, platinum complex should have a *cis* geometry. The general formula of the complex should be *cis*-$[PtX_2(Am)_2]$. In the formula, X represents leaving group and most of the time Cl is used. Am represents inert amines which can be *mono*- or *bi*-dentate and there should be at least one N-H component [39][40]. Finally, the complex should have diamine or related compounds as a non-leaving bridging reagent to have a chelating effect [41].

Additionally, it is known that d^8 transition metals can be used in the area of ligand substitution, *cis/trans* isomerization, and catalytic processes such as isomerization, polymerization when they have five coordination [42]. It is also suggested that they can be used as protecting groups for the olefin derivatives stabilization. Since platinum is a d^8 transition metal too, all these possibilities can be explored with platinum [43, 44].

1.7. Synthetic Routes to Quinoxaline Structure

Most of quinoxaline derivatives can be synthesized from quinoxalin-2-ones by using well-known oxidation and reduction procedures (Figure 1.4.) [45].

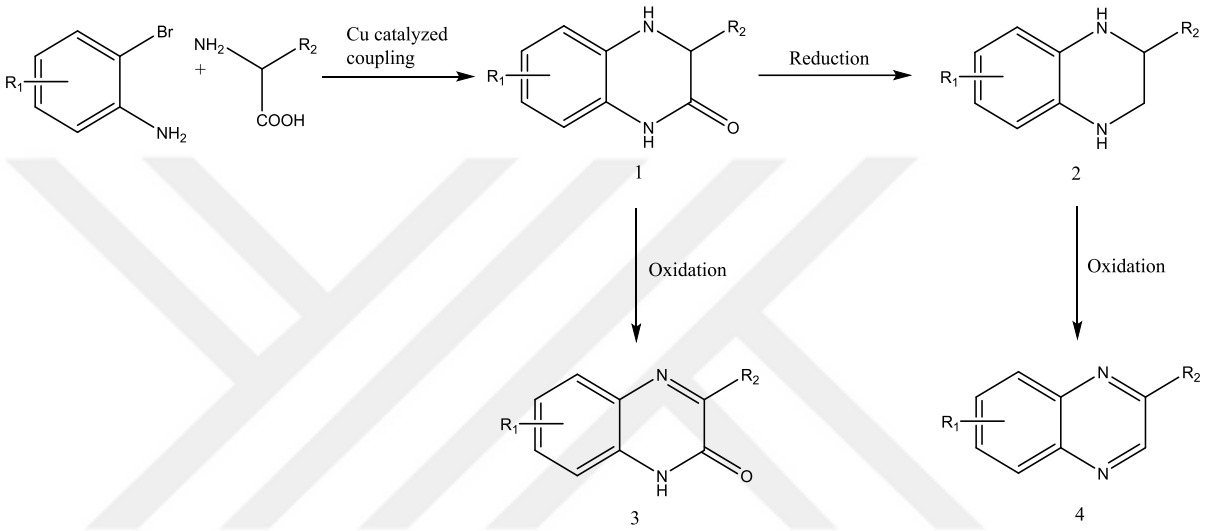


Figure 1.4. Synthetic Approach for Quinoxalinones 1, 1,2,3,4-Tetrahydroquinoxalines 2, Quinoxalines 3, and Quinoxalin-2(1H)-ones 4 [45].

There has been a wide range of research to find new and effective synthetic routes for the syntheses of quinoxalines. However, Körner and Hinsberg method is the most used one. The condensation of *o*-phenylenediamine with reactive 1,2-dicarbonyl compounds (e.g. 1,2-diketones, 1,2 ketoesters or oxalic acid derivatives) is called as Körner and Hinsberg method. Also there are examples of many catalysts and reagents such as molecular iodine, ionic liquids, sulfamic or heteropoly acids, modified silica gel, polyaniline sulfate salts, cerium ammonium nitrate which are used for the construction of quinoxalines in the literature [46]. Additionally, mechanochemical methods are also used for the synthesis of this heteroaromatic system currently [47].

2. AIM OF THE STUDY

Quinoxaline derivatives are used in photovoltaics, optoelectronic devices, flame resistant polymers and they have a wide range of biological applications. They can be used as fluorophores, photosensitizer, corrosion inhibitor, and electron-transport material. The application of platinum complexes is possible for the therapy of tumors, C-H activating catalysts and supporting materials in conversion of solar energy area. They are also electrochemically active and have applications in the area of cis/trans isomerization, and catalytic processes such as isomerization, polymerization as mentioned in introduction [31]. Thus, platinum complexes with quinoxaline derivatives are our interest in view of their different chemical and electronical features. It was aimed to optimize the syntheses of two different functionalized quinoxalines as potential redox active ligands and synthesize their platinum complexes. Physical and chemical characterization of newly synthesized molecules were investigated *via* ^{1}H and ^{13}C NMR, DSC, fluorescent and UV-Vis spectrophotometer.

3. EXPERIMENTAL

3.1. Methods and Materials

All chemicals were used as received from the manufacturer (Merck, Aldrich, Alfa Aesar, Acros Organics, and Riedel de Haen). All reactions and work-up procedures were carried out under an argon atmosphere by using Schlenk technique except work-up procedure of N^9, N^9, N^{10}, N^{10}-tetramethylacenaphtho [1, 2-b] quinoxaline-9, 10-diamine.

3.2. Instrumentation

^{1}H-NMR and ^{13}C-NMR were recorded by using a Varian Gemini 400 MHz spectrometer at the Advanced Technologies Research and Development Center at Boğaziçi University. All UV-Vis spectra were measured with the UV-2401 PC (Schimadzu) UV spectrophotometer. Fluorescence spectra were recorded in ethanol solvent and done by Cary Eclipse fluorescence spectrophotometer. Thermal characterization of molecules were measured by EXSTAR SII DSC 7020 instrument. Cyclic voltammetry was carried out in 0.1 molar Bu_4NPF_6 solution using a three electrode configuration (glassy carbon working electrode, Ag/AgCl reference) and a PAR 273 potentiostat and function generator at University of Stuttgart. The ferrocene/ ferrocenium (Fc/Fc+) couple served as internal reference.

3.3. Synthesis of the Ligands

3.3.1. Synthesis of Acenaphtho [1,2-b] quinoxaline-9, 10-diamine

Acenaphtho [1,2-b] quinoxaline-9, 10-diamine was synthesized through the condensation reaction of 1,2,4,5-Benzenetetramine tetrahydrochloride and acenaphthenequinone. By using Schlenk technique under an argon atmosphere, 1,2,4,5-Benzenetetramine tetrahydrochloride (10.224 mg, 0.36 mmol), acenaphthenequinone (65.58 mg, 0.36 mmol) and potassium carbonate (99.36 mg, 0.72 mmol) were added to the reaction flask. 150 mL EtOH and 15 mL water were added as solvents to the reaction. The temperature of reaction was kept at 65℃ for 3 days. The reaction mixture was filtered; filtrate part was collected and precipitated into 1:3 v/v EtOH:H_2O mixture. Product was dried for 4 hours under high vacuum. The final product was obtained as a yellow solid with 85% yield (Figure 3.1.). ^{1}H NMR (400 MHz, acetone) δ 8.08 (d, *J* = 6.9 Hz, 2H), 7.95 (d, *J* = 8.3 Hz, 2H), 7.69 (dd, *J* = 8.3, 6.9 Hz, 2H), 7.16 (s, 2H), 5.06 (s, 4H). ^{13}C NMR (400 MHz,THF) δ (Ar*C*) 149.51, (Ar*C*) 140.50, 138.20, (Ar*C*) 134.08, (Ar*C*) 129.95, (Ar*C*) 128.08, (Ar*C*) 127.35, (Ar*C*) 119.62, (Ar*C*) 108.94 ppm.

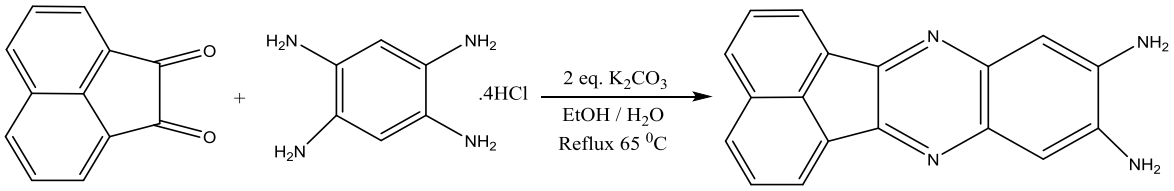


Figure 3.1. Synthesis of Acenaphtho [1, 2-b] quinoxaline-9, 10-diamine.

3.3.2. Synthesis of Acenaphtho [1, 2-b] quinoxaline-9, 10-diamine dihydrochloride

Acenaphtho [1, 2-b] quinoxaline-9, 10-diamine dihydrochloride was synthesized through the condensation reaction of 1,2,4,5-Benzenetetramine tetrahydrochloride and acenaphthenequinone. By using Schlenk technique under an argon atmosphere, 1,2,4,5-Benzenetetramine tetrahydrochloride (10.224 mg, 0.36 mmol), acenaphthenequinone (65.58 mg, 0.36 mmol) and potassium carbonate (49.68 mg, 0.36 mmol) were added to the reaction flask. 150 mL EtOH and 15 mL water were added as solvents to the reaction. The temperature of reaction was kept at 65℃ for 3 days. The reaction mixture was filtered; filtrate part was collected and precipitated into 1:3 ratio EtOH:H_2O mixture. Product was dried for 4 hours by using high vacuum. The final product was dark red solid obtained with 83% yield (Figure 3.2.). ^{1}H NMR (400 MHz, d_8THF) δ 8.05 (d, *J* = 7.0 Hz, 2H), 7.85 (d, *J* = 8.6 Hz, 2H), 7.65 – 7.57 (t, 2H), 7.04 (s, 2H). ^{13}C NMR (400 MHz, d_8THF) δ (Ar*C*) 151.40, (Ar*C*) 142.36, (Ar*C*) 140.02, (Ar*C*) 135.94, (Ar*C*) 131.77, (Ar*C*) 129.93, (Ar*C*) 129.28, (Ar*C*) 121.51, (Ar*C*) 110.74 ppm.

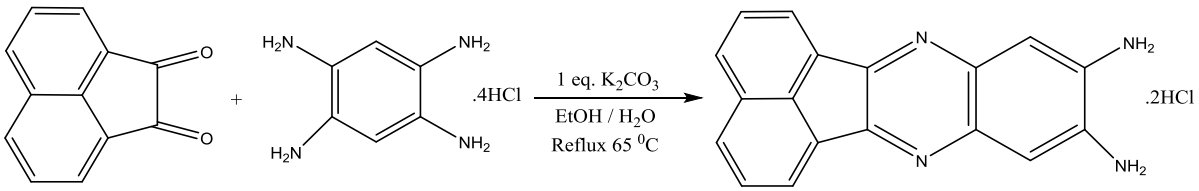


Figure 3.2. Synthesis of Acenaphtho [1, 2-b] quinoxaline-9, 10-diamine dihydrochloride.

3.3.3. Synthesis of N^9, N^9, N^{10}, N^{10}-tetramethylacenaphtho [1, 2-b] quinoxaline-9, 10-diamine

By using Schlenk technique under an argon atmosphere, acenaphtho [1, 2-b] quinoxaline-9, 10-diamine dihydrochloride (80 mg, 0.225 mmol) and paraformaldehyde (68 mg, 2.246 mmol) were added to the reaction flask with 8 mL of glacial acetic acid. Sodium cyanoborohydride was dissolved in 5 mL acetic acid and added to the reaction flask drop wise. Reaction flask was kept in an ice bath and left overnight. In an open atmosphere, the reaction mixture was filtered and filtrate part was collected. Product was dark brown solid. Dark brown solid was dissolved in 30 mL EtOAc and extracted with 30 ml Brine and 30 ml $NaHCO_3$, respectively. The organic layer was dried over Na_2SO_4, filtered and put in a vacuum oven. The final product was dark brown solid obtained with 80% yield (Figure 3.3.). ^{1}H NMR (400 MHz, $CDCl_3$) δ 8.26 (d, *J* = 7.0 Hz, 2H), 7.93 (d, *J* = 8.2 Hz, 2H), 7.75 – 7.65 (t, 2H), 7.19 (s, 2H), 2.91 (s, 12H). ^{13}C NMR (400 MHz, $CDCl_3$) δ (Ar*C*) 175.45, (Ar*C*) 151.44, (Ar*C*) 148.62, (Ar*C*) 138.22, (Ar*C*) 135.04, (Ar*C*) 132.48, (Ar*C*) 129.74, (Ar*C*) 128.49, (Ar*C*) 120.98, (Ar*C*) 114.83, (*C*H_3) 41.47 ppm.

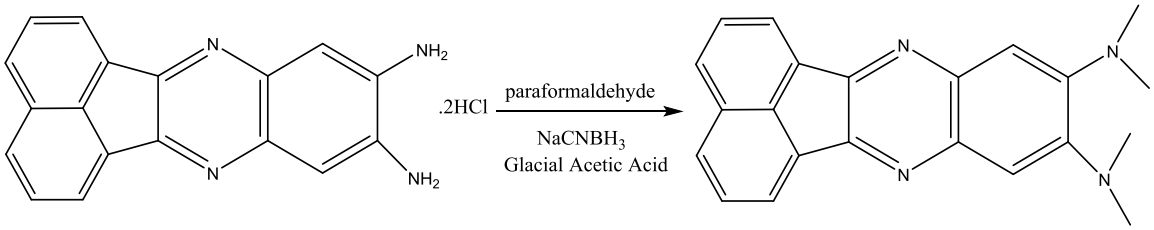


Figure 3.3. Synthesis of N9, N9, N10, N10-tetramethylacenaphtho [1, 2-b] quinoxaline-9, 10-diamine.

3.4. Synthesis of the Complexes

3.4.1. Synthesis of Acenaphtho [1, 2-b] quinoxaline-9, 10-diamine Platinum Complex

$Pt(DMSO)_2Cl_2$ salt was prepared by using a literature procedure [48]. By using Schlenk technique under argon atmosphere, acenaphtho [1, 2-b] quinoxaline-9, 10-diamine (80 mg, 0.281 mmol) was dissolved in 17 mL MeCN in the reaction flask. $Pt(DMSO)_2Cl_2$ (180 mg, 0.360 mmol) was dissolved in 10 mL MeCN and added dropwise to the reaction flask. Temperature of the reaction was kept at 40℃ and the reaction was carried out overnight. The reaction mixture was filtered and filtrate part was collected. The product was dark yellow solid (Figure 3.4.). ^{1}H NMR (400 MHz, CD_3CN) δ 8.46 (d, *J* = 7.0 Hz, 2H), 8.32 (d, *J* = 8.3 Hz, 2H), 8.22 (s, 1H), 8.14 (s, 1H), 7.98 (dd, *J* = 8.3, 7 Hz, 2H), 6.9 (br, 2H).

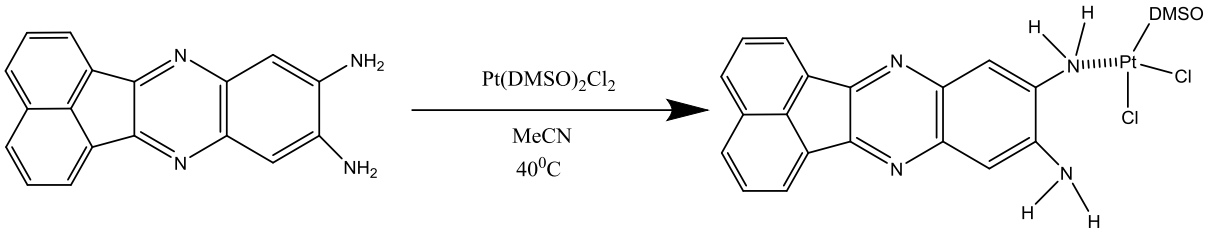


Figure 3.4. Synthesis of Acenaphtho [1, 2-b] quinoxaline-9, 10-diamine Platinum Complex.

3.4.2. Synthesis of N^9, N^9, N^{10}, N^{10}-tetramethylacenaphtho [1, 2-b] quinoxaline-9, 10-diamine Platinum Complex

$Pt(DMSO)_2Cl_2$ salt was prepared by using a literature procedure [48]. By using Schlenk technique under argon atmosphere, N^9, N^9, N^{10}, N^{10}-tetramethylacenaphtho [1, 2-b]

quinoxaline-9, 10-diamine (60 mg, 0.176 mmol) was dissolved in 15 mL MeCN in reaction flask. $Pt(DMSO)_2Cl_2$ (74.32 mg, 0.176 mmol) was dissolved in 10 mL MeCN and added dropwise to the reaction flask. The reaction flask was left overnight at 40℃. There was not any precipitation. Evaporation of the solvent gave the final product as a dark red solid which could not be further purified (Figure 3.5.).

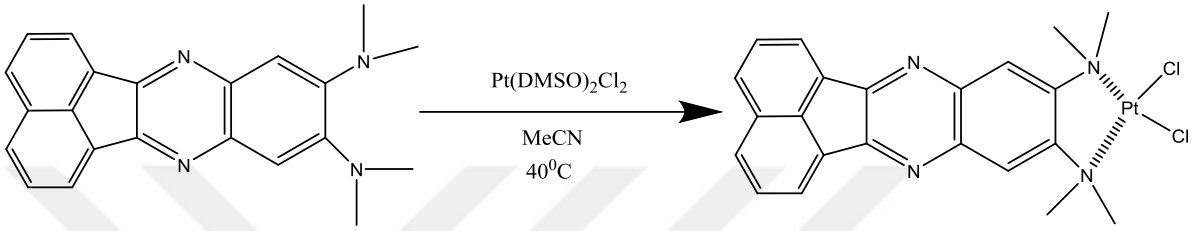


Figure 3.5. Synthesis of N^9, N^9, N^{10}, N^{10}-tetramethylacenaphtho [1, 2-b] quinoxaline-9, 10-diamine Platinum Complex.

4. RESULTS AND DISCUSSION

In this study, the syntheses of two functionalized quinoxaline ligands were optimized and then the coordination of the ligands to a platinum metal center were studied. There have been two proposed synthetic routes to synthesize both of the ligands [49]. The first route was for the acenaphtho [1, 2-b] quinoxaline-9, 10-diamine synthesis (L1). It was direct coupling of 1, 2, 4, 5-Benzenetetramine tetrahydrochloride to acenaphthenequinone through a condensation reaction in water and ethanol. The second route, which is a methylation reaction, was for N^9, N^9, N^{10}, N^{10}-tetramethylacenaphtho [1, 2-b] quinoxaline-9, 10-diamine (L2).

4.1. Syntheses of Acenaphtho [1, 2-b] quinoxaline-9, 10-diamine and Acenaphtho [1, 2-b] quinoxaline-9, 10-diamine dihydrochloride

Acenaphtho [1, 2-b] quinoxaline-9, 10-diamine (Figure 3.1.) is a yellow solid product. During the work-up procedure, it was observed that the color changes from yellow to brown within few seconds. The product decomposes when it is exposed to the air. Decomposition occurs as a consequence of oxidation of the amines in the structure. Thus all the experiments and work-up procedure were done under argon in the Schlenk system in an air free environment. In addition, the amount of solvent was increased to make the reaction medium more dilute. In that way, intramolecular cyclization was made favorable (Figure 4.1.). Moreover, the reaction time was increased from 1 day to 3 days in order to decrease the amount of kinetic product, which was seen as impurity, and obtain the desired thermodynamic product. As a result, the yield was increased from 12% to 85%.

The same procedure was used to obtain acenaphtho [1, 2-b] quinoxaline-9, 10-diamine dihydrochloride (Figure 3.2.). Acenaphtho [1, 2-b] quinoxaline-9, 10-diamine dihydrochloride is a dark red solid. Its solubility in water is better than acenaphtho [1, 2-b] quinoxaline-9, 10-diamine. In the last step of the work-up procedure, precipitation of the

product into water was not easy like in the case of acenaphtho [1, 2-b] quinoxaline-9, 10-diamine. Thus, more time was needed for the precipitation of the product. As a result the yield was 83%.

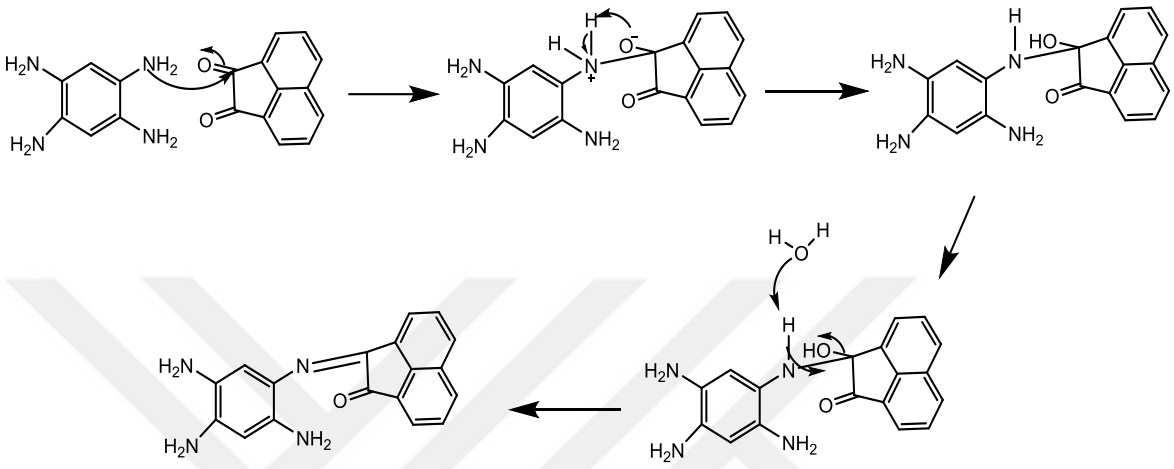


Figure 4.1. Mechanism of Acenaphtho [1, 2-b] quinoxaline-9, 10-diamine Reaction.

4.2. Synthesis of N^9, N^9, N^{10}, N^{10}-tetramethylacenaphtho [1, 2-b] quinoxaline-9, 10-diamine

In the synthesis of N^9, N^9, N^{10}, N^{10}- tetramethylacenaphtho [1, 2-b] quinoxaline-9, 10-diamine, acenaphtho [1, 2-b] quinoxaline-9, 10-diamine dihydrochloride was used instead of acenaphtho [1, 2-b] quinoxaline-9, 10-diamine.

In order to have the attack of diamines to formaldehyde molecule, the medium has to be acidic according to reaction mechanism. When glacial acetic acid was added to acenaphtho [1, 2-b] quinoxaline-9, 10-diamine, it was observed that the color of the ligand changed from yellow to dark red. The change of the color was the same when amines in acenaphtho [1, 2-b] quinoxaline-9, 10-diamine molecule was protonated. It was thought that protons from glacial acetic acid were used to protonate the amines in acenaphtho [1, 2-b]

quinoxaline-9, 10-diamine, not for the reaction medium. However, the acidic medium is necessary to run the reaction in high yield (Figure 4.2.). In order to obtain an acidic medium, the protonation of acenaphtho [1, 2-b] quinoxaline-9, 10-diamine was done from the beginning. As a result, the product was obtained without any side product and that shortened the work up procedure. The yield was increased from 34% to 80%.

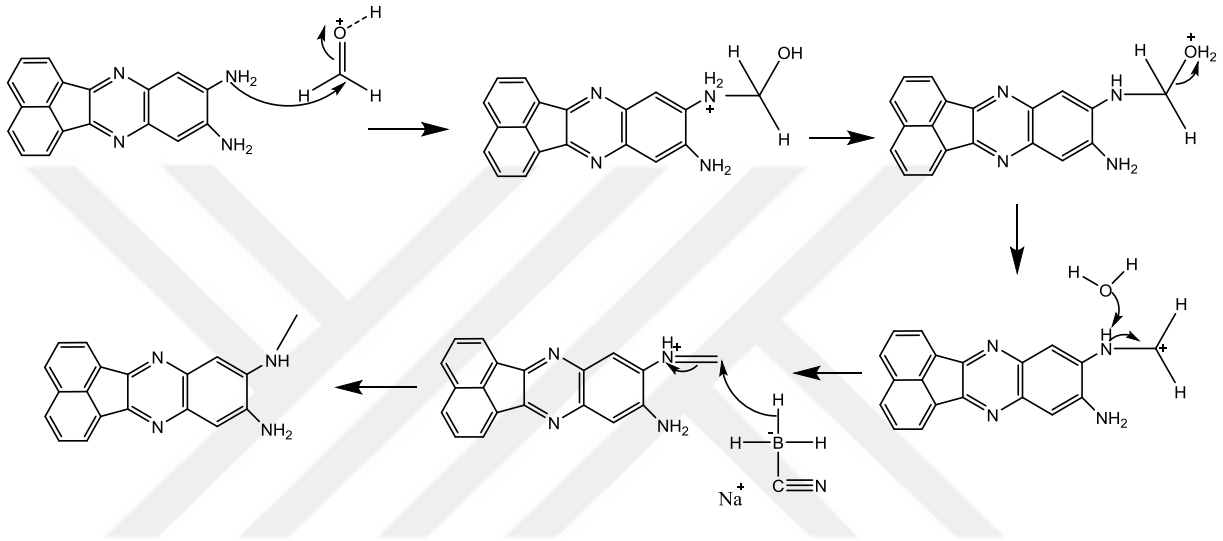


Figure 4.2. Mechanism of N9, N9, N10, N10- tetramethylacenaphtho [1, 2-b] quinoxaline-9, 10-diamine Reaction.

4.3. Synthesis of Acenaphtho [1, 2-b] quinoxaline-9, 10-diamine Platinum Complex

Both of the ligands were used to synthesize platinum complexes. $Pt(DMSO)_2Cl_2$ was used as the platinum source. The formation of the complexes were investigated *via* ^1H NMR spectroscopy.

In the ^1H NMR spectrum of acenaphtho [1, 2-b] quinoxaline-9, 10-diamine platinum complex, it was observed that all H peaks on the ligand were shifted to lower field. The effect of complexation of the platinum with the nitrogen atoms can be observed by the downfield shift of the N-H signals in ^1H NMR spectrum. The displacement of the signals to

higher chemical shifts indicates the existence of the complexation of the platinum. The complexation causes reduction in the electron density on the ligand. Unfortunately, the expected ^{195}Pt satellites caused by ^{195}Pt-H coupling was not observed in the spectrum of the complex, due to broadening of the newly formed signal at 6.9 ppm [50, 51].

In the ^{1}H NMR spectrum of the complex, H_c doublet was shifted from 8.13 ppm to 8.46 ppm (Figure A.8). H_a doublet was shifted from 8.00 ppm to 8.32 ppm. H_b triplet was shifted from 7.75 ppm to 7.98 ppm. Amine peaks of the ligand were shifted from 5.37 ppm to 6.92 ppm. H_d peak was a singlet in ligand ^{1}H NMR. However it was seen as two different signals in the complex spectrum. They were also shifted to lower field upon complexation by the platinum. Moreover, methyl peak with platinum satellites was observed at 3.5 ppm. It came from the unreacted $Pt(DMSO)_2Cl_2$ that was given in excess amount at the beginning. The signal at 2.5 ppm is due to the released DMSO after complexation. Another peak 2.47 ppm with satellites leads to the assumption that platinum is coordinated only to one NH_2 of the Quinoxaline structure. The integration of the peak at 2.47 ppm gives the ratio of 3:1 (Methyl peaks of coordinated DMSO : $2H_d$ protons of the ligand). The different magnetic environments of H_a and H_a', H_b and H_b', H_c and H_c' cannot be differentiated in the mono-substituted complex well due to the overlapping of the doublets and triplets of the aromatic region. However the broadening of these multiples can be taken as an evidence for their nonsymmetrical behavior (Figure 4.3.). Crystallization of the complex was tried to get a single crystal but could not be succeeded.

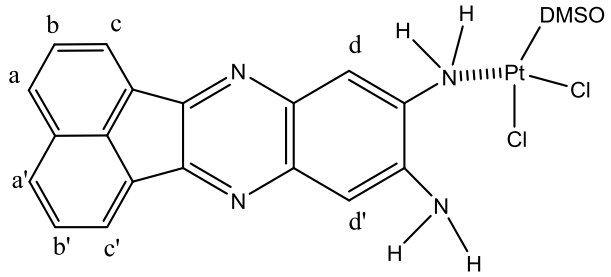


Figure 4.3. Acenaphtho [1, 2-b] quinoxaline-9, 10-diamine Platinum complex structure.

4.4. Synthesis of N^9, N^9, N^{10}, N^{10}-tetramethylacenaphtho [1, 2-b] quinoxaline-9, 10-diamine Platinum Complex

In the reaction of N^9, N^9, N^{10}, N^{10}- tetramethylacenaphtho [1, 2-b] quinoxaline-9, 10-diamine with $Pt(DMSO)_2Cl_2$, ^1H NMR spectrum cannot be used to explain the formation of a pure platinum complex. Although there were some downfield shifts in the aromatic region, indicative of complex formation, the ^1H NMR spectrum was too complicated to be resolved. However thermal analysis, UV-Vis and Fluorescence Spectra show the presence of a new platinum complex.

4.5. UV - Vis Spectra of Synthesized Molecules

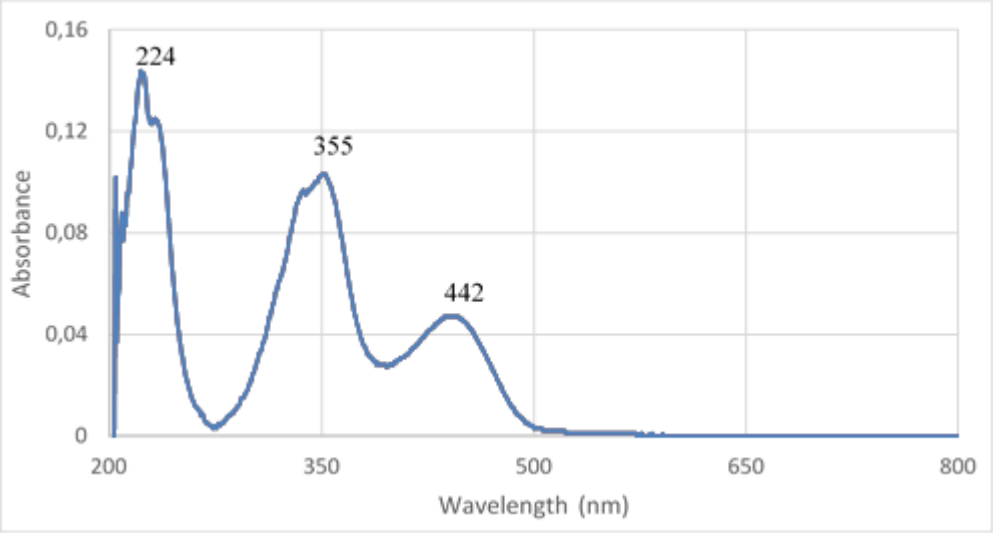


Figure 4.4. UV – Vis Spectrum of acenaphtho [1, 2-b] quinoxaline-9, 10-diamine.

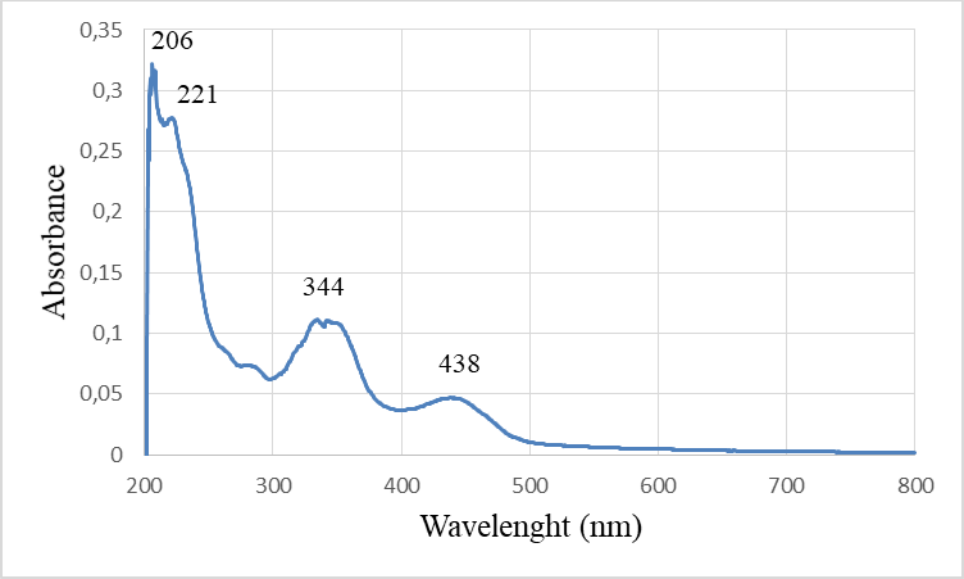


Figure 4.5. UV – Vis Spectrum of acenaphtho [1, 2-b] quinoxaline-9, 10-diamine dihydrochloride.

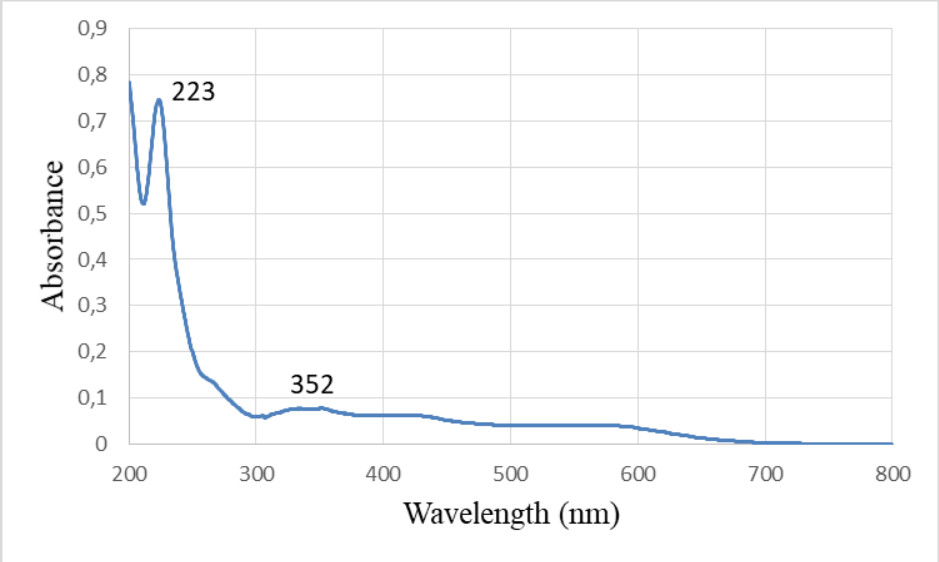


Figure 4.6. UV – Vis Spectrum of acenaphtho [1, 2-b] quinoxaline-9, 10-diamine Platinum Complex.

According to UV-Vis Spectra, it can be seen that there is a small change in between UV-Vis Spectra of acenaphtho [1, 2-b] quinoxaline-9, 10-diamine (Figure 4.4.) and acenaphtho [1, 2-b] quinoxaline-9, 10-diamine platinum complex (Figure 4.6.) which can be

attributed to the ligand to metal charge transfer. It can be also seen that acenaphtho [1, 2-b] quinoxaline-9, 10-diamine dihydrochloride UV-Vis spectrum does not show any similarity with the formed platinum complex (Figure 4.5.).

As we compare UV-Vis Spectra of N^9, N^9, N^{10}, N^{10}- tetramethylacenaphtho [1, 2-b] quinoxaline-9, 10-diamine (Figure 4.7.) and N^9, N^9, N^{10}, N^{10}- tetramethylacenaphtho [1, 2-b] quinoxaline-9, 10-diamine platinum complex (Figure 4.8.), the difference between the two spectra in the region above 400 nm is caused possibly by the ligand to metal charge transfer.

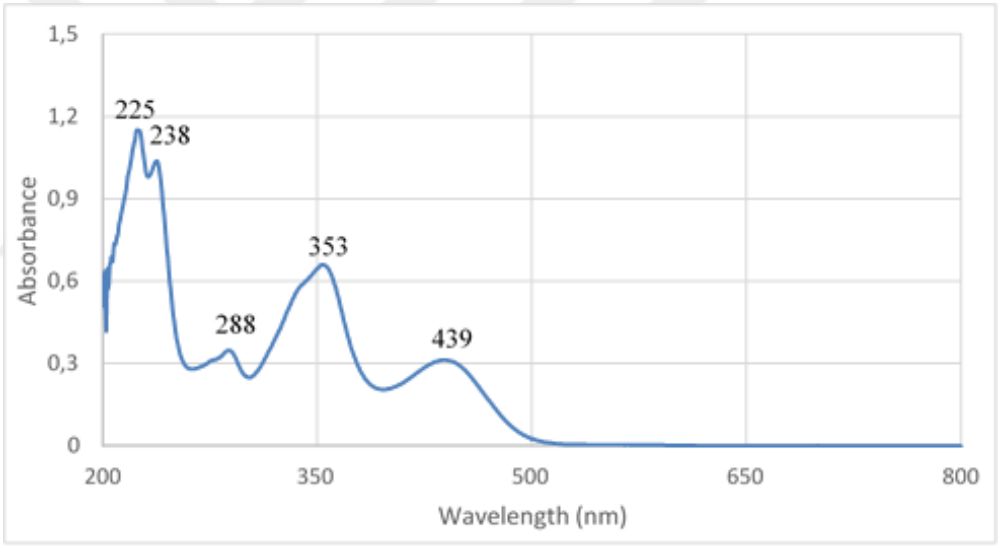


Figure 4.7. UV – Vis Spectrum of N^9, N^9, N^{10}, N^{10}- tetramethylacenaphtho [1, 2-b] quinoxaline-9, 10-diamine.

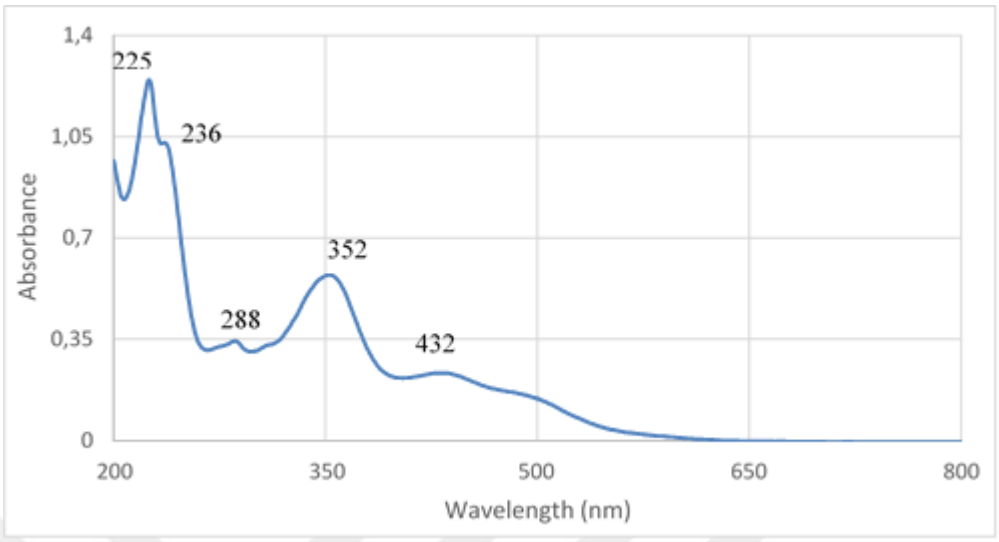


Figure 4.8. UV – Vis Spectrum of N^9, N^9, N^{10}, N^{10}- tetramethylacenaphtho [1, 2-b] quinoxaline-9, 10-diamine Platinum Complex.

4.6. Fluorescence Spectra of Synthesized Molecules

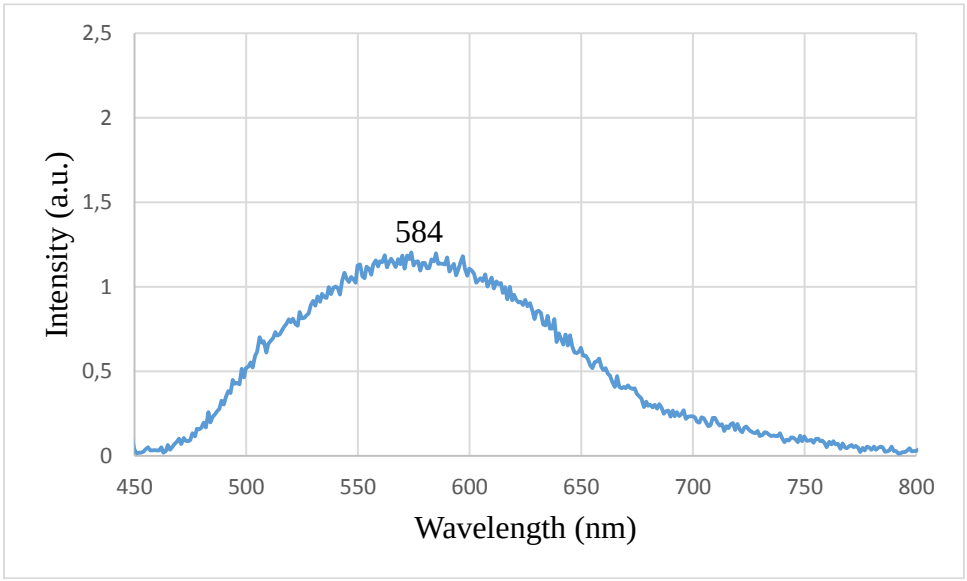


Figure 4.9. Fluorescence Spectrum of acenaphtho [1, 2-b] quinoxaline-9, 10-diamine (activation λ = 442 nm).

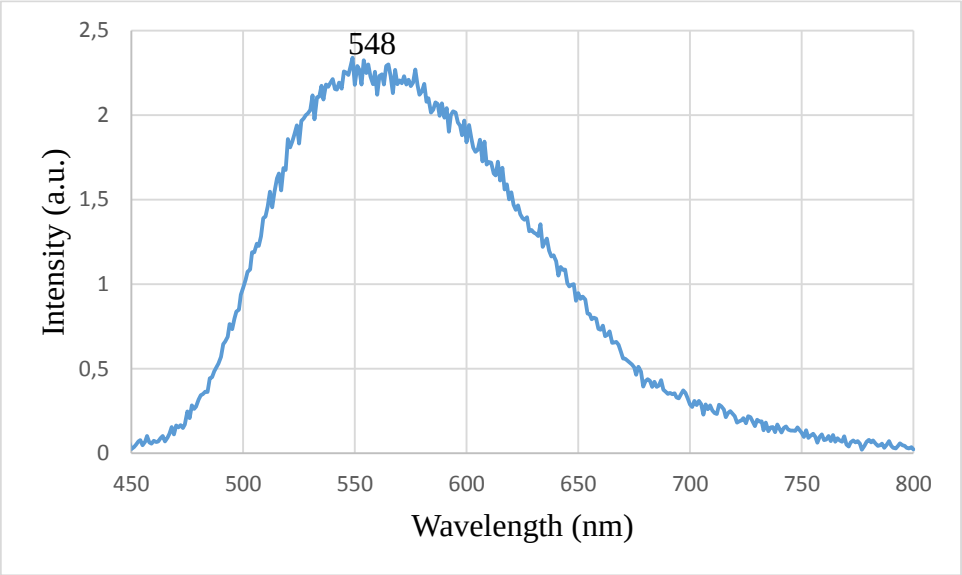


Figure 4.10. Fluorescence Spectrum of acenaphtho [1, 2-b] quinoxaline-9, 10-diamine dihydrochloride (activation λ = 438 nm).

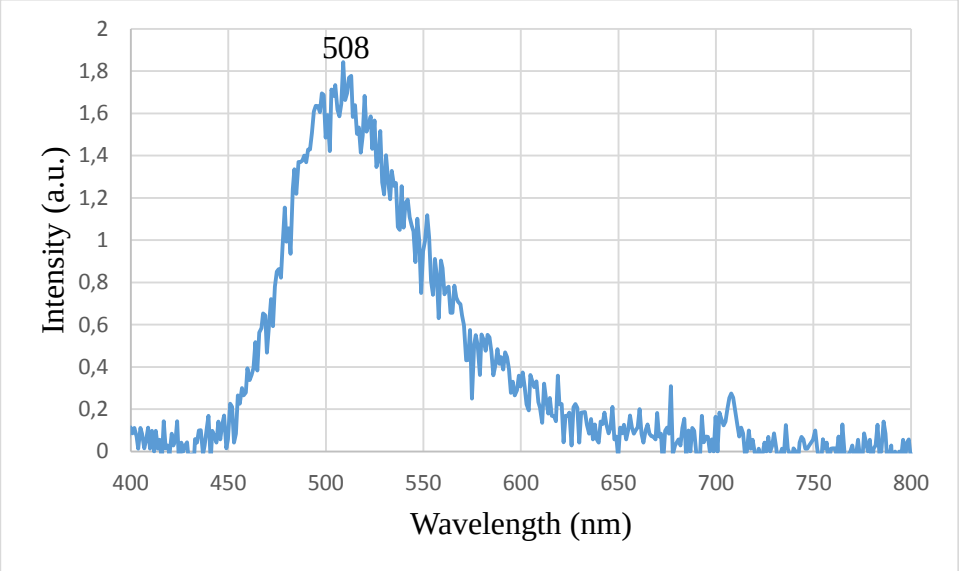


Figure 4.11. Fluorescence Spectrum of acenaphtho [1, 2-b] quinoxaline-9, 10-diamine Platinum Complex (activation λ = 354 nm).

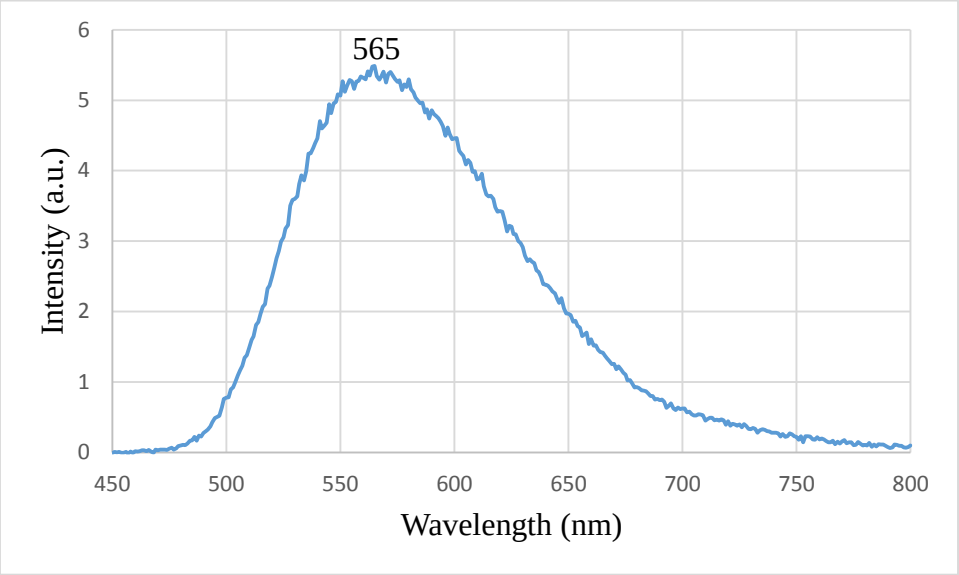


Figure 4.12. Fluorescence Spectrum of N^9, N^9, N^{10}, N^{10}- tetramethylacenaphtho [1, 2-b] quinoxaline-9, 10-diamine (activation λ = 439 nm).

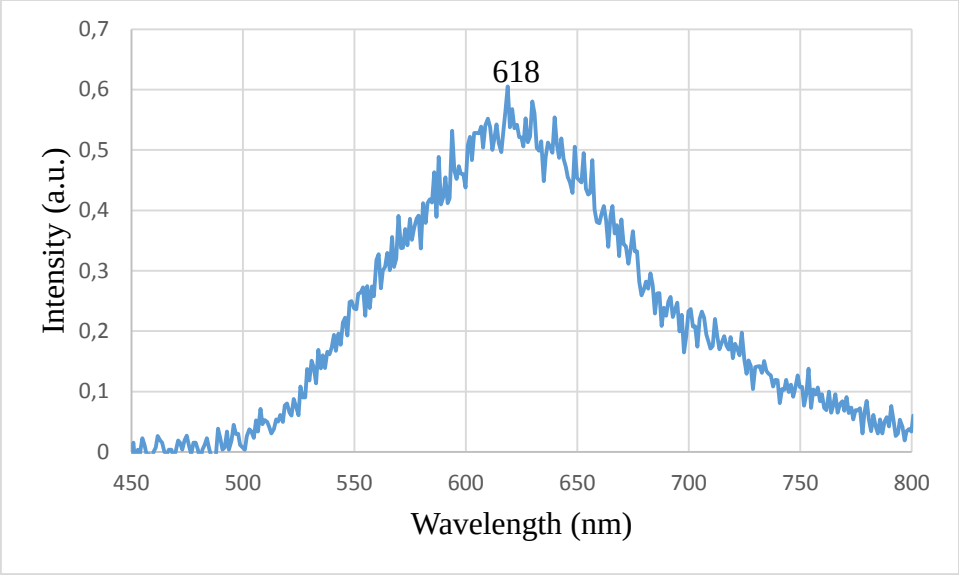


Figure 4.13. Fluorescence Spectrum of N^9, N^9, N^{10}, N^{10}- tetramethylacenaphtho [1, 2-b] quinoxaline-9, 10-diamine Platinum Complex (activation λ = 432 nm).

As reported by fluorescence spectra, acenaphtho [1, 2-b] quinoxaline-9, 10-diamine, acenaphtho [1, 2-b] quinoxaline-9, 10-diamine dihydrochloride and N^9, N^9, N^{10}, N^{10}-

tetramethylacenaphtho [1, 2-b] quinoxaline-9, 10-diamine show fluorescence at 584, 548 and 565 nm respectively (Figures 4.9, 4.10, 4.12), whereas the platinum complexes of these ligands show fluorescence at 508 and 618 nm (Figures 4.11., 4.13.).

4.7. Cyclic Voltammetry Analysis of the Synthesized Molecules

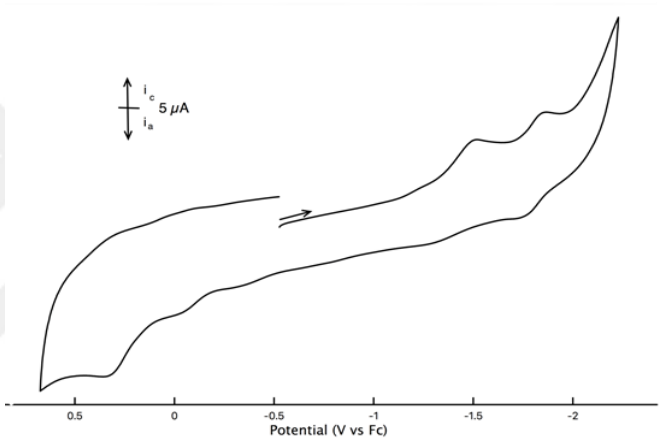


Figure 4.14. Cyclic Voltammogram of Acenaphtho [1, 2-b] quinoxaline-9, 10-diamine.

Cyclic voltammogram of Acenaphtho [1, 2-b] quinoxaline-9, 10-diamine was obtained in acetonitrile (Figure 4.14). According to the voltammogram, reduction wave tends to be reversible at around -2 volt but the presence of amino groups cause oxidation during the analysis. Thus, a clear voltammogram could not be obtained.

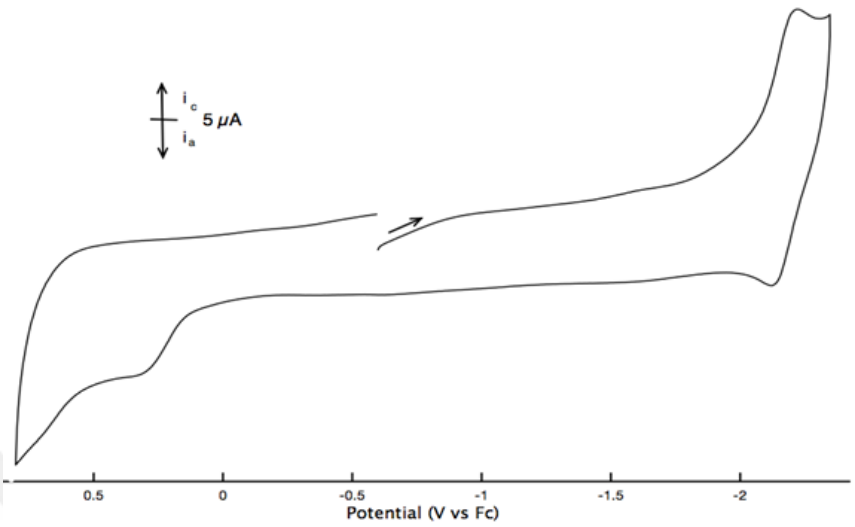


Figure 4.15. Cyclic Voltammogram of Acenaphtho [1, 2-b] quinoxaline-9, 10-diamine dihydrochloride.

Cyclic voltammogram of Acenaphtho [1, 2-b] quinoxaline-9, 10-diamine dihydrochloride was also obtained in acetonitrile (Figure 4.15.). However the solvent was not suitable for this measurement range. Another solvent with a reduction potential beyond -2 volts should be used. However due to the poor solubility of the ligand in other solvents clear cyclic voltammogram of the ligand could not be obtained.

4.8. Thermal Analysis of Synthesized Molecules

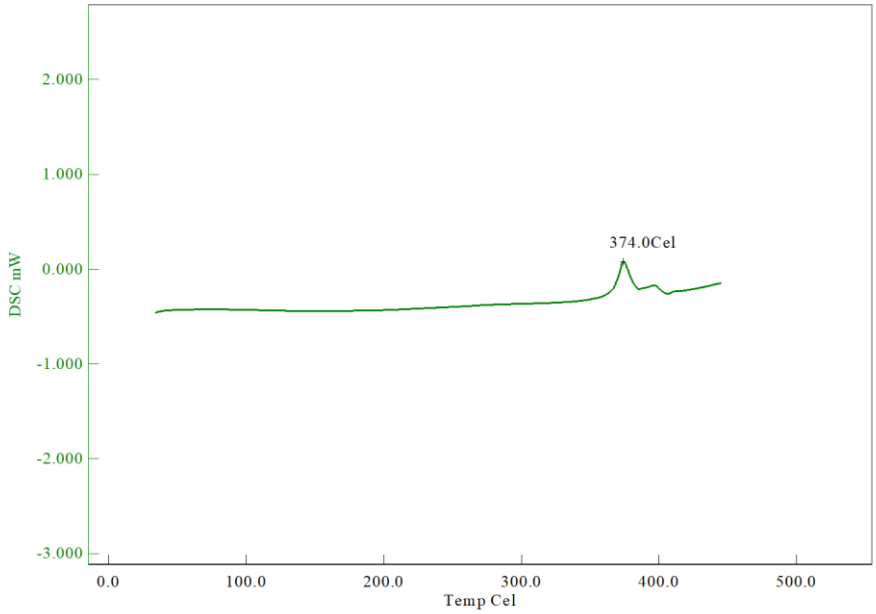


Figure 4.16. DSC Spectrum of acenaphtho [1, 2-b] quinoxaline-9, 10-diamine.

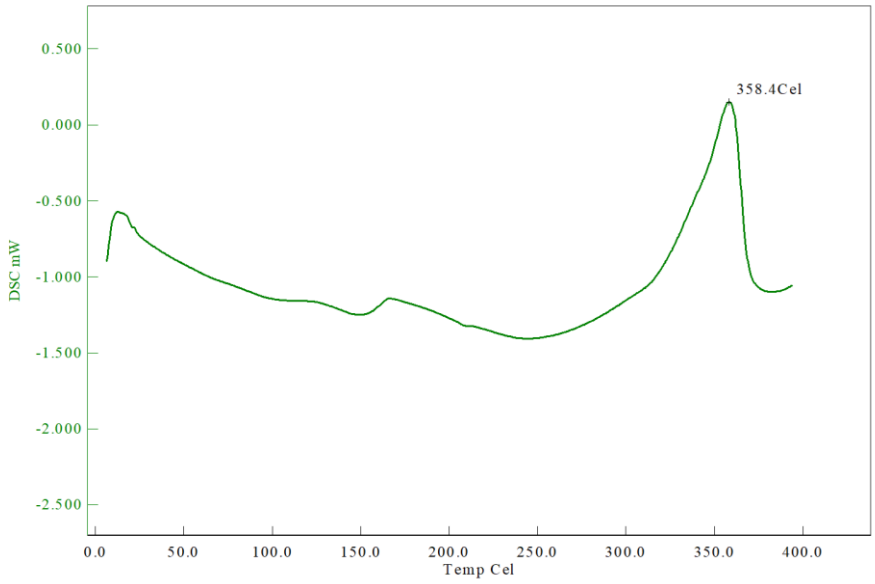


Figure 4.17. DSC Spectrum of acenaphtho [1, 2-b] quinoxaline-9, 10-diamine dihydrochloride.

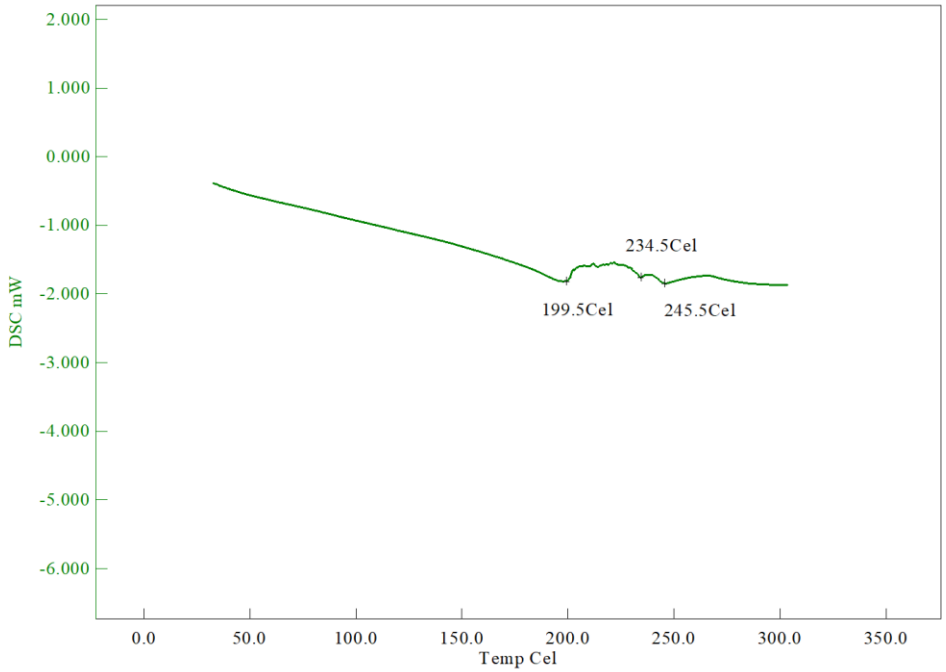


Figure 4.18. DSC Spectrum of acenaphtho [1, 2-b] quinoxaline-9, 10-diamine Platinum Complex.

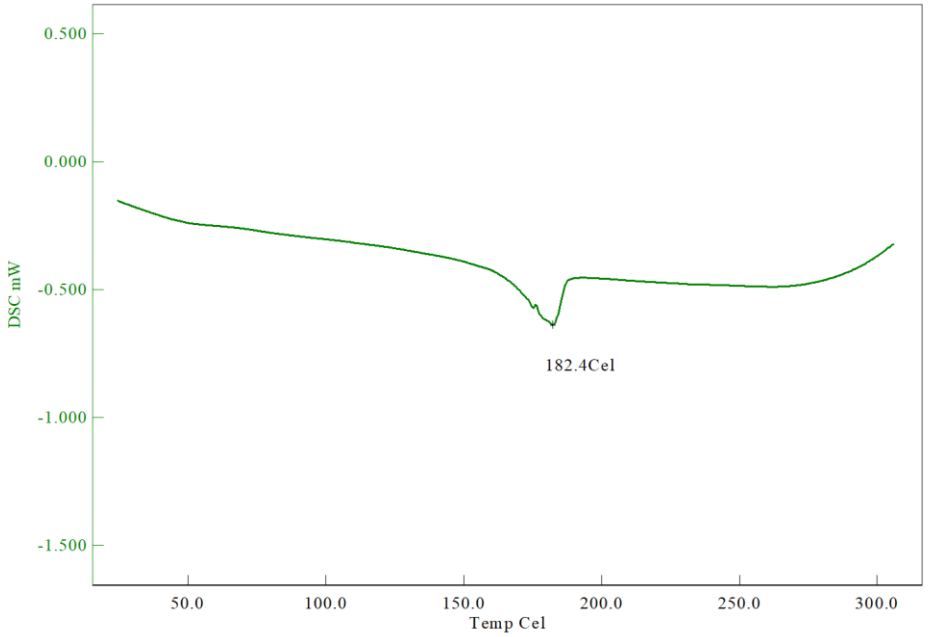


Figure 4.19. DSC Spectrum of N^9, N^9, N^{10}, N^{10}- tetramethylacenaphtho [1, 2-b] quinoxaline-9, 10-diamine.

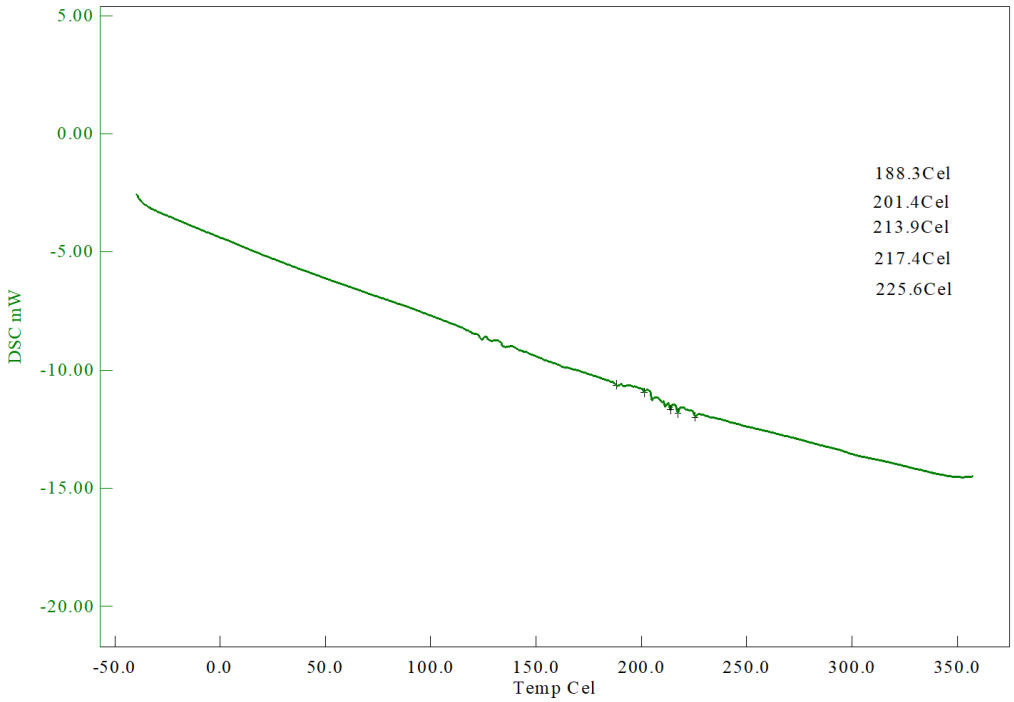


Figure 4.20. Spectrum of N^9, N^9, N^{10}, N^{10}- tetramethylacenaphtho [1, 2-b] quinoxaline-9, 10-diamine platinum complex.

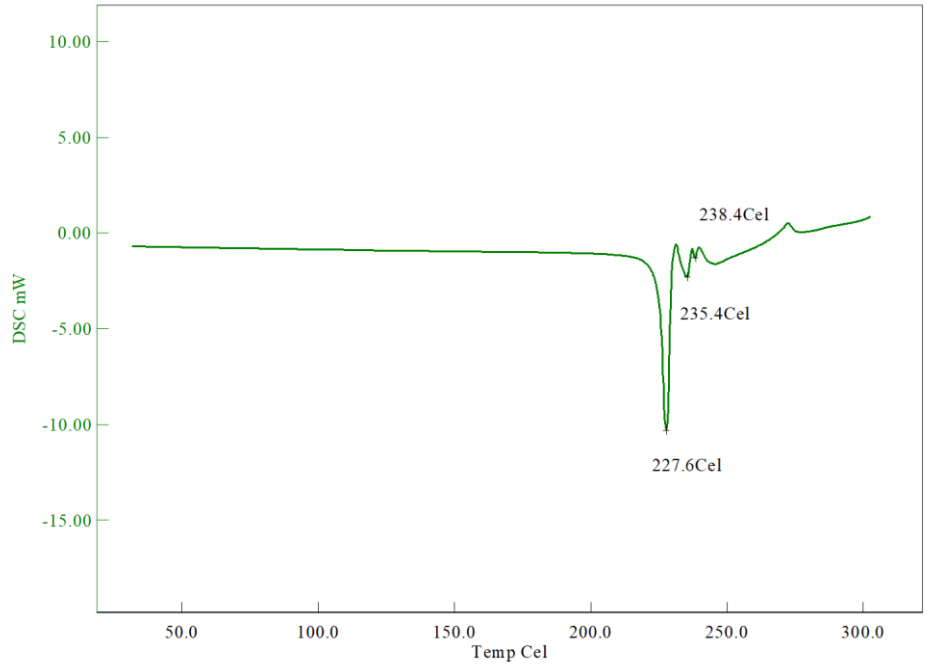


Figure 4.21. DSC Spectrum of $PtCl_2(DMSO)_2$.

According to DSC analysis, acenaphtho [1, 2-b] quinoxaline-9, 10-diamine and acenaphtho [1, 2-b] quinoxaline-9, 10-diamine dihydrochloride decompose before melting (Figure 4.16., 4.17.).

Table 4.1. Melting Points of the Synthesized Compounds according to DSC Results.

Name of the Compound	Melting Point of the Compound
Acenaphtho [1, 2-b] quinoxaline-9, 10-diamine	Decomposes before melting
Acenaphtho [1, 2-b] quinoxaline-9, 10-diamine dihydrochloride	Decomposes before melting
Acenaphtho [1, 2-b] quinoxaline-9, 10-diamine Platinum Complex	199.5℃
N^9, N^9, N^{10}, N^{10}- tetramethylacenaphtho [1, 2-b] quinoxaline-9, 10-diamine	182.4℃
N^9, N^9, N^{10}, N^{10}- tetramethylacenaphtho [1, 2-b] quinoxaline-9, 10-diamine Platinum Complex	201.4℃
cis-Dichlorobis(dimethyl sulfoxide)platinum(II)	227.6℃

According to thermal analysis, acenaphtho [1, 2-b] quinoxaline-9, 10-diamine platinum complex was synthesized. Its melting point is 199.5℃ (Figure 4.18.). Peaks other than the complex melting point belong to unreacted $Pt(DMSO)_2Cl_2$ salt (Figure 4.21.). The results are consistent with ^1H NMR spectra. Also, it can be seen that N^9, N^9, N^{10}, N^{10}- tetramethylacenaphtho [1, 2-b] quinoxaline-9, 10-diamine melting point is 182.4℃ (Figure 4.19.).

N^9, N^9, N^{10}, N^{10}- tetramethylacenaphtho [1, 2-b] quinoxaline-9, 10-diamine platinum complex has a melting point at 201.4℃ (Figure 4.20.). Peaks other than the complex melting point belong to unreacted $Pt(DMSO)_2Cl_2$ salt and N^9, N^9, N^{10}, N^{10}- tetramethylacenaphtho [1, 2-b] quinoxaline-9, 10-diamine (Table 4.1.).

5. CONCLUSIONS

In this study, the yield optimization of two different functionalized quinoxalines as potential redox active ligands and syntheses of their platinum complexes were investigated. According to results, syntheses of the ligands were optimized and platinum complexes of the ligands were synthesized. Coordination was observed from thermal, ^{1}H NMR and fluorescence spectroscopic analyses for both of the complexes. However, the complexes could not be obtained as pure products. Physical and chemical characterization of the synthesized ligands and complexes were determined *via* ^{1}H and ^{13}C NMR, DSC, fluorescent and UV-Vis spectrophotometer. It was shown that both of these ligands can act as ligands to transition metals the first example was with platinum.

6. FUTURE WORK

As future work, the complexes will be purified and crystallized to obtain single crystal of them. Their elemental composition, crystal and grain structures will be investigated *via* X-ray analysis. Electrochemical analysis of the synthesized molecules will be performed by using cyclic voltammetry. Also, synthesized ligands will be examined for the coordination of other transition metal centers.

REFERENCES

1. J. A. Pereira *et al.*, “Quinoxaline, its derivatives and applications: A State of the Art review,” *Eur. J. Med. Chem.*, vol. 97, pp. 664–672, 2015.

2. A. K. Patidar, M. Jeyakandan, A. K. Mobiya, and G. Selvam, “Exploring potential of quinoxaline moiety,” *Int. J. PharmTech Res.*, vol. 3, no. 1, pp. 386–392, 2011.

3. A. A. Abu-Hashem, “Synthesis, Reactions and Biological Activity of Quinoxaline Derivatives.,” *Am. J. Org. Chem.*, vol. 5, no. 1, pp. 14–56, 2015.

4. C. Tong *et al.*, “Bisacenaphthopyrazinoquinoxaline derivatives: synthesis, physical properties and applications as semiconductors for n-channel field effect transistors.,” *Org. Biomol. Chem.*, vol. 11, no. 34, pp. 5683–91, 2013.

5. A. V. Tsukanov, A. D. Dubonosov, V. A. Bren, and V. I. Minkin, “Organic chemosensors with crown-ether groups (review),” *Chem. Heterocycl. Compd.*, vol. 44, no. 8, pp. 899–923, 2008.

6. C. K. Jang and J. Y. Jaung, “The Synthesis and Optical Properties of Fluorescent Quinoxalines and of Electrospun Fibers Containing Fluorescent Quinoxaline,” *J. Nanosci. Nanotechnol.*, vol. 11, no. 1, pp. 494–498, 2011.

7. J. Y. Jaung, “Synthesis and halochromism of new quinoxaline fluorescent dyes,” *Dye. Pigment.*, vol. 71, no. 3, pp. 245–250, 2006.

8. S. Yamaguchi, S. Akiyama, and K. Tamao, “Photophysical Properties Changes Caused by Hypercoordination of Organosilicon Compounds : From Trianthrylfluorosilane to Trianthryldifluorosilicate Modification of π -electron systems by the main group elements represents a new direction toward the constr,” *J. Am. Chem. Soc.*, no. 8, pp. 6793–6794, 2000.

9. D. W. Chang, S. J. Ko, J. Y. Kim, L. Dai, and J. B. Baek, “Multifunctional quinoxaline containing small molecules with multiple electron-donating moieties: Solvatochromic

and optoelectronic properties," *Synth. Met.*, vol. 162, no. 13–14, pp. 1169–1176, 2012.

10. Z. El Adnani *et al.*, "Investigation of newly pyridazine derivatives as corrosion inhibitors in molar hydrochloric acid. Part III: Computational calculations," *Int. J. Electrochem. Sci.*, vol. 7, no. 5, pp. 3982–3996, 2012.

11. I. B. Obot and N. O. Obi-Egbedi, "2,3-Diphenylbenzoquinoxaline: A new corrosion inhibitor for mild steel in sulphuric acid," *Corros. Sci.*, vol. 52, no. 1, pp. 282–285, 2010.

12. E. E. Ebenso *et al.*, "Quantum Chemical Investigations on Quinoline Derivatives as Effective Corrosion Inhibitors for Mild Steel in Acidic Medium," *Int. J. Electrochem. Sci. Int. J. Electrochem. Sci*, vol. 7, no. 7, pp. 5643–5676, 2012.

13. B. Yan, Q. Ma, Y. Wang, and J. Chen, "Synthesis, characterisation and antibacterial activity of ZnS–ZnO nanocomposites," *Mater. Technol.*, vol. 7857, no. September, pp. 1–6, 2016.

14. L. A. Berben, B. de Bruin, and A. F. Heyduk, "Non-innocent ligands," *Chem. Commun.*, vol. 51, no. 9, pp. 1553–1554, 2015.

15. H. Kotani, T. Sugiyama, T. Ishizuka, Y. Shiota, K. Yoshizawa, and T. Kojima, "Redox-Noninnocent Behavior of Tris(2-pyridylmethyl)amine Bound to a Lewis Acidic Rh(III) Ion Induced by C-H Deprotonation," *J. Am. Chem. Soc.*, vol. 137, no. 35, pp. 11222–11225, 2015.

16. J. I. Van Der Vlugt and J. N. H. Reek, "Neutral tridentate PNP ligands and their hybrid analogues: Versatile non-innocent scaffolds for homogeneous catalysis," *Angew. Chemie - Int. Ed.*, vol. 48, no. 47, pp. 8832–8846, 2009.

17. V. Lyaskovskyy and B. De Bruin, "Redox non-innocent ligands: Versatile new tools to control catalytic reactions," *ACS Catal.*, vol. 2, no. 2, pp. 270–279, 2012.

18. P. J. Chirik, "Preface : Forum on Redox-Active Ligands," *Inorg. Chem.*, vol. 50 , no. 20, pp. 9737–9740, 2011.

19. W. Kaim and B. Schwederski, “Non-innocent ligands in bioinorganic chemistry-An overview,” *Coord. Chem. Rev.*, vol. 254, no. 13–14, pp. 1580–1588, 2010.

20. R. Eisenberg and H. B. Gray, “Noninnocence in metal complexes: A dithiolene dawn,” *Inorg. Chem.*, vol. 50, no. 20, pp. 9741–9751, 2011.

21. C. K. Jorgensen, “Differences between the four halide ligands, and discussion remarks on trigonal-bipyramidal complexes, on oxidation states, and on diagonal elements of one-electron energy,” *Coord. Chem. Rev.*, vol. 1, no. 1, pp. 164–178, 1966.

22. W. Kaim, “Manifestations of noninnocent ligand behavior,” *Inorg. Chem.*, vol. 50, no. 20, pp. 9752–9765, 2011.

23. M. D. Ward and J. a. McCleverty, “Non-innocent behaviour in mononuclear and polynuclear complexes: consequences for redox and electronic spectroscopic properties,” *J. Chem. Soc. Dalt. Trans.*, no. 3, pp. 275–288, 2002.

24. K. P. Butin, E. K. Beloglazkina, and N. V Zyk, “Metal complexes with non-innocent ligands,” *Russ. Chem. Rev.*, vol. 74, no. 6, pp. 531–553, 2005.

25. A. J. Hartshorn, “Ligand design and synthesis,” *Coordination Chemistry Reviews*, vol. 9, pp. 219–274, 1973.

26. E. C. Constable and P. J. Steel, “N,N'-Chelating biheteroaromatic ligands; a survey,” *Coord. Chem. Rev.*, vol. 93, no. 2, pp. 205–223, 1989.

27. C. J. Dhanaraj and J. Johnson, “Metal Complexes of Quinoxaline Derivatives : Review (Part-I),” *Research Journal of Chemical Sciences*, vol. 4, no. 11, pp. 80–102, 2014.

28. Bernhard Lipper, *Cisplatin*, Verlag Helvetica Chimica Acta, Zurich, Switzerland, 1999.

29. S. Roy *et al.*, “Phenanthroline derivatives with improved selectivity as DNA-targeting anticancer or antimicrobial drugs,” *ChemMedChem*, vol. 3, no. 9, pp. 1427–1434, 2008.

30. P. Svoboda, T. S. Belopotapova, and J. Hetflejš, “Catalysis by metal complexes,” *J. Organomet. Chem.*, vol. 65, no. 2, pp. C37–C38, 1974.

31. P. Du *et al.*, “Bi- and terpyridyl platinum(II) chloro complexes: Molecular catalysts for the photogeneration of hydrogen from water or simply precursors for colloidal platinum,” *J. Am. Chem. Soc.*, vol. 130, no. 15, pp. 5056–5058, 2008.

32. W. Kaim *et al.*, “Reduced and excited states of (bpym)[PtCl2]n (bpym = 2,2′-bipyrimidine; n = 1, 2): Experiments and DFT calculations,” *Inorg. Chem.*, vol. 41, no. 16, pp. 4139–4148, 2002.

33. M. Kato, A. Omura, A. Toshikawa, S. Kishi, and Y. Sugimoto, “Vapor-induced luminescence switching in crystals of the Syn isomer of a dinuclear (bipyridine)platinum(II) complex bridged with pyridine-2-thiolate ions,” *Angew. Chemie - Int. Ed.*, vol. 41, no. 17, pp. 3183–3185, 2002.

34. L. P. Moorcraft *et al.*, “Synthesis and properties of [Pt(4-CO(2)CH(3)-py)(2)(mnt)]: comparison of pyridyl and bipyridyl-based dyes for solar cells.,” *Dalton Trans.*, vol. 2, no. 48, pp. 6940–7, 2008.

35. R. Büchner, C. T. Cunningham, J. S. Field, R. J. Haines, D. R. McMillin, and G. C. Summerton, “Luminescence properties of salts of the [Pt(4′Ph-terpy)Cl]+ chromophore: crystal structure of the red form of [Pt(4′Ph-terpy)Cl]BF4 (4′Ph-terpy = 4′-phenyl-2,2′:6′,2″-terpyridine),” *J. Chem. Soc. Dalt. Trans.*, vol. 4, no. 5, pp. 711–718, 1999.

36. S. R. Seidel and P. J. Stang, “High-symmetry coordination cages via self-assembly,” *Acc. Chem. Res.*, vol. 35, no. 11, pp. 972–983, 2002.

37. E. Bulak *et al.*, “2,3-Bis(1-methylimidazol-2-yl)quinoxaline (bmiq), a new ligand with decoupled electron transfer and metal coordination sites: the very different redox behaviour of isoelectronic complexes with $[PtCl_2]$ and $[AuCl_2]^+$.,” *Dalton Trans.*, vol. 40, no. 12, pp. 2757–63, 2011.

38. M. J. Cleare and J. D. Hoeschele, “Studies on the antitumor activity of group VIII transition metal complexes. Part I. Platinum (II) complexes,” *Bioinorg. Chem.*, vol. 2, no. 3, pp. 187–210, 1973.

39. M. V. De Almeida, J. D. S. Chaves, A. P. S. Fontes, E. T. César, and M. Gielen, “Synthesis and characterization of platinum(II) complexes from trifluoromethyl phenylenediamine, picoline and N-benzyl ethylenediamine derivatives,” *J. Braz. Chem. Soc.*, vol. 17, no. 7, pp. 1266–1273, 2006.

40. P. Jia *et al.*, “Review: recent advances and future development of metal complexes as anticancer agents,” *J. Coord. Chem.*, vol. 8972, no. June, pp. 1–27, 2017.

41. P. J. Bednarski, “Reactions of a cisplatin analog bearing an estrogenic 1,2-diarylethylenediamine ligand with sulfur-containing amino acids and glutathione,” *J. Inorg. Biochem.*, vol. 60, no. 1, pp. 1–19, 1995.

42. Cotton F., Wilkinson G., Murillo C., Bochmann M., *Advanced Inorganic Chemistry*, John Wiley & Sons, Inc., New York, NY, USA, 6th edition, 1999.

43. F. Giordano *et al.*, “Stabilization of unstable unsaturated molecules in five-coordinate TBP complexes of Pt (II): vinyl alcohol derivatives,” *J. Organomet. Chem.*, vol. 264, no. II, pp. 231–237, 1997.

44. M. Benedetti, D. Antonucci, C. R. Girelli, and F. P. Fanizzi, “Hindrance, Donor Ability of Me n ∩ NN Chelates and Overall Stability of Pentacoordinate [PtCl 2 (η 2 -CH 2 =CH 2)(Me n ∩ NN)] Complexes as Observed by η 2 -Olefin 1 J Pt,C Modulation: An NMR Study,” *Eur. J. Inorg. Chem.*, vol. 2015, no. 13, pp. 2308–2316, 2015.

45. S. Tanimori, “Sequential Synthesis, Olfactory Properties, and Biological Activity of Quinoxaline Derivatives,” *ACS Omega*, vol. 2, no. 5, pp. 1875-1885, 2017.

46. Z. T. Bhutia, G. Prasannakumar, A. Das, and M. Biswas, “z Sustainable Chemistry A Facile , Catalyst-Free Mechano-Synthesis of Quinoxalines and their In-Vitro Antibacterial Activity Study,” *Chemistry Select*, vol. 2, pp. 1183–1187, 2017.

47. P. K. Sahoo, C. Giri, S. Haldar, and R. Puttreddy, “Mechanochemical Synthesis , Photophysical Properties , and X-ray Structures of N-Heteroacenes,” *Eur. J. Org. Chem*, vol. 2016, no. 7, pp. 1283–1291, 2016.

48. R. Romeo, L. M. Scolaro, V. Catalano, and S. Achar, “(2,2′: 6′,2″-Terpyridine)Methylplatinum(II) Chloride and (1,10-Phenanthroline)-Methylchloroplatinum(II),” *Inorg. Synth.*, vol. 32, pp. 153–158, 1998.

49. A. Aykanat, “Synthesis of and Characterization of Precursor for Quinoxaline Cyclization,” Ms, Institute for Graduate Studies for Science and Engineering, Boğaziçi University, 2015.

50. M. D. Anker, M. Arrowsmith, R. L. Arrowsmith, M. S. Hill, and M. F. Mahon, “Alkaline-Earth Derivatives of the Reactive $[HB(C_6F_5)_3]^-$ Anion,” *Inorg. Chem*, vol. 3, no. 96, pp. 6009–6014, 1996.

51. R. Ettorre and A. Gambaro, “^{1}H and ^{13}C NMR Studies of Palladimn (I1) and Platinum (II) Complexation of Cytosine,” *Journal of Magnetic Resonance*, vol. 457, no. 22, pp. 453–457, 1976.

APPENDIX A: SPECTROSCOPY DATA

This section includes ^{1}D NMR (^{1}H, ^{13}C NMR) spectroscopy of the synthesized products. Expansions were made on the NMR data for easy interpretation.

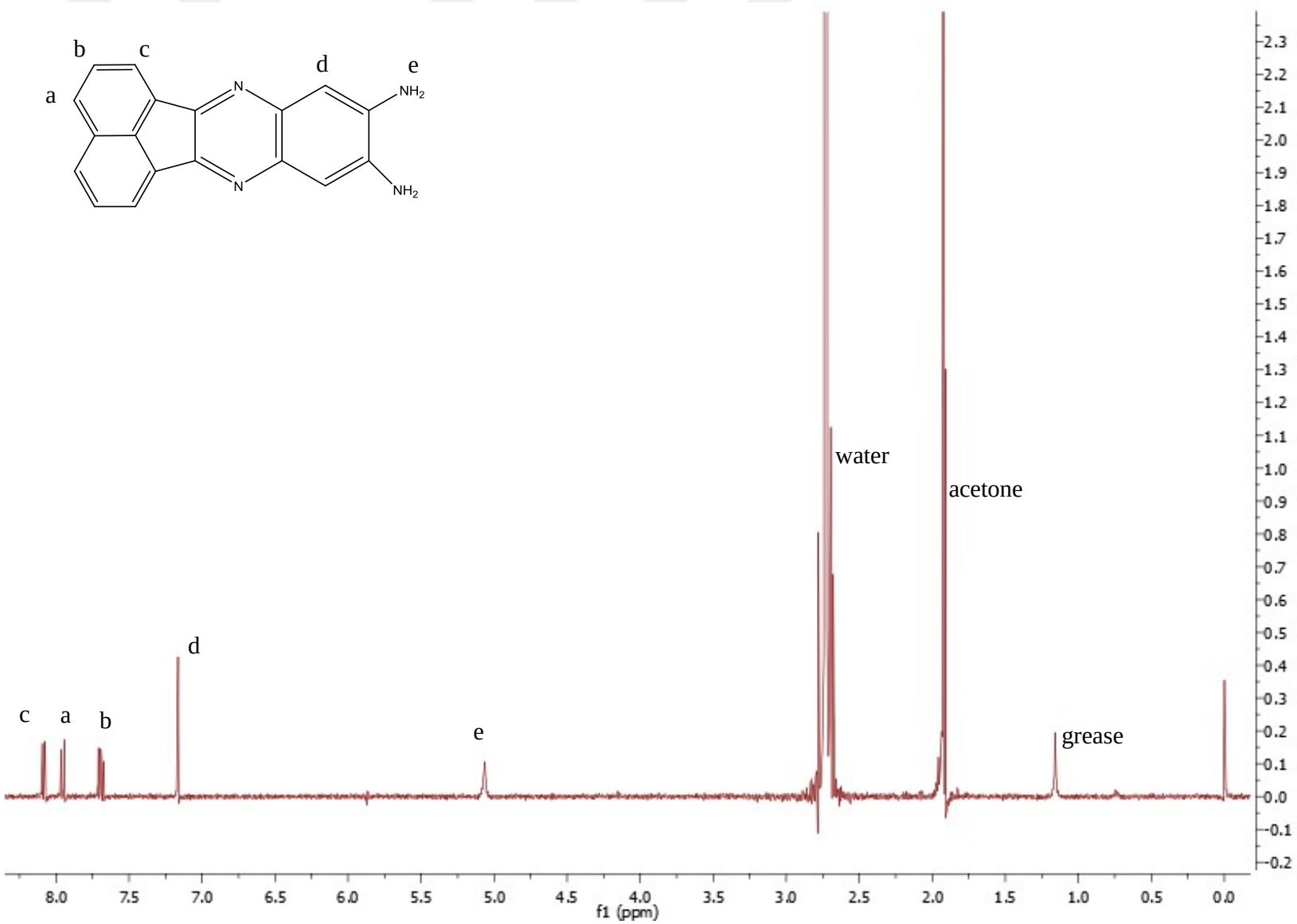


Figure A.1. ^{1}H-NMR Spectrum of Acenaphtho [1, 2-b] quinoxaline-9, 10-diamine in $(CD_3)_2CO$.

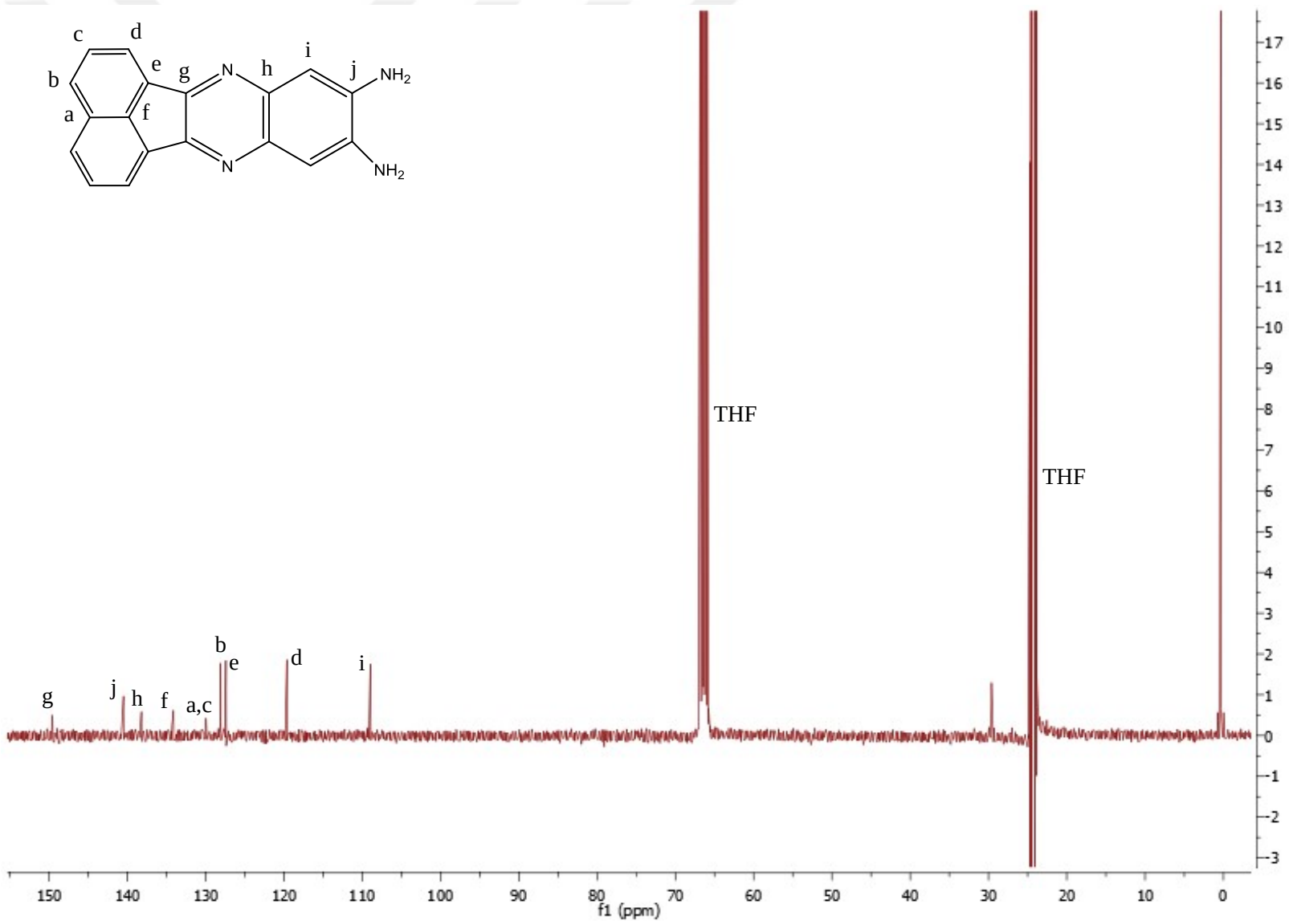


Figure A.2. ^{13}C-NMR Spectrum of Acenaphtho [1, 2-b] quinoxaline-9, 10-diamine in d_8THF.

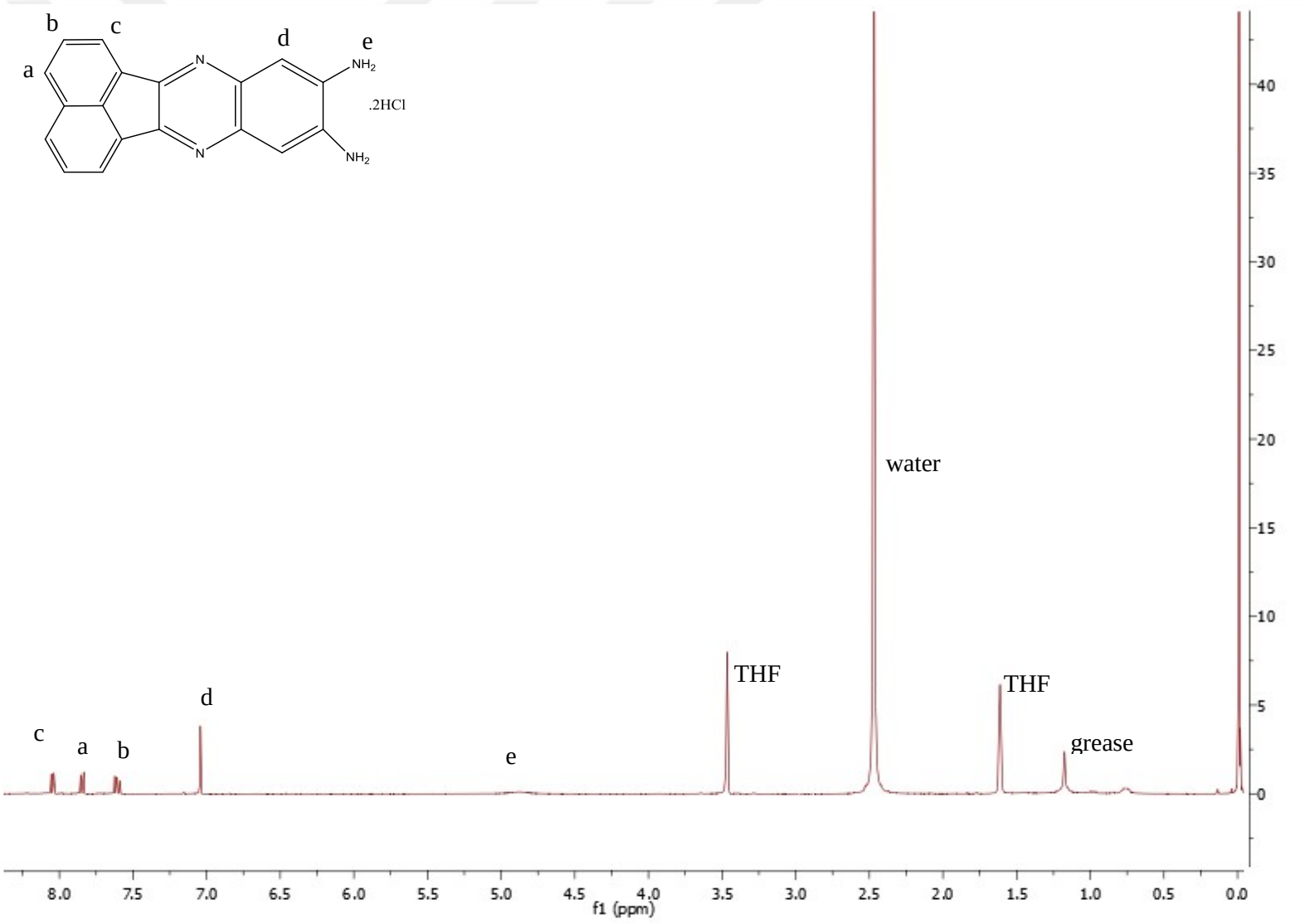


Figure A.3. ^{1}H-NMR Spectrum of Acenaphtho [1, 2-b] quinoxaline-9, 10-diamine dihydrochloride in d_8THF.

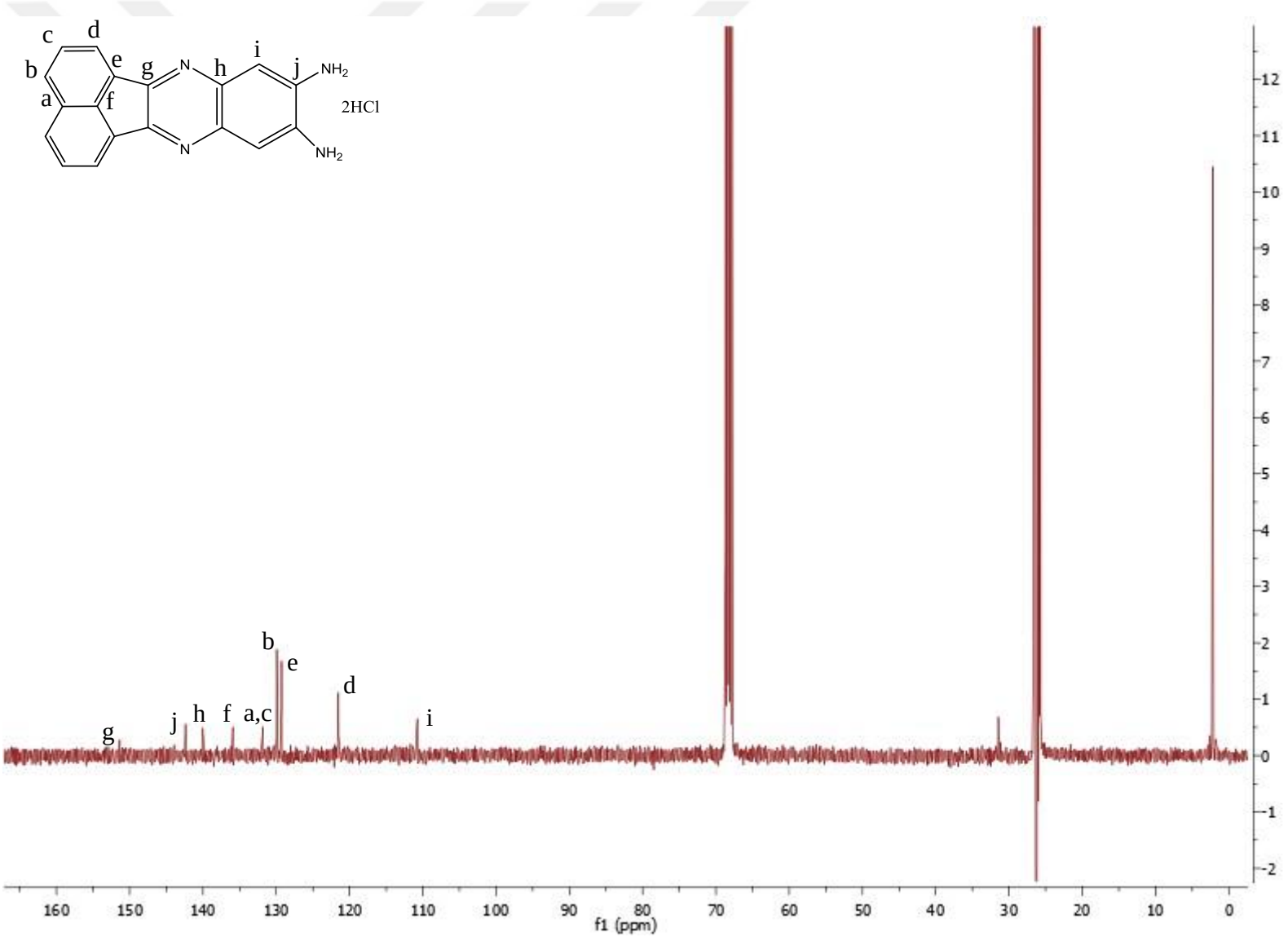


Figure A.4. ^{13}C-NMR Spectrum of Acenaphtho [1, 2-b] quinoxaline-9, 10-diamine dihydrochloride in d_8THF.

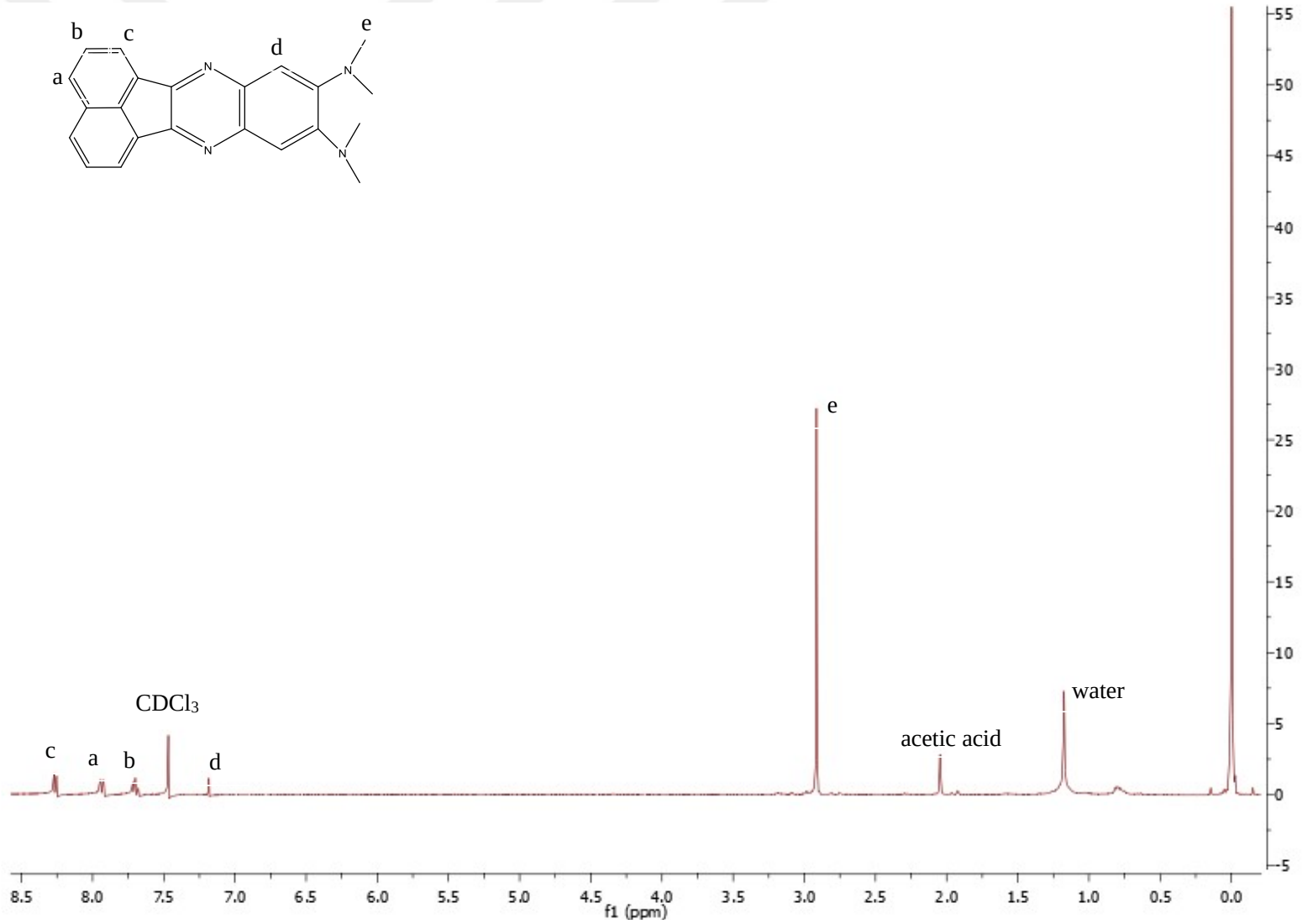


Figure A.5. ^{1}H-NMR Spectrum of N^{9}, N^{9}, N^{10}, N^{10}- tetramethylacenaphtho [1, 2-b] quinoxaline-9, 10-diamine in $CDCl_3$.

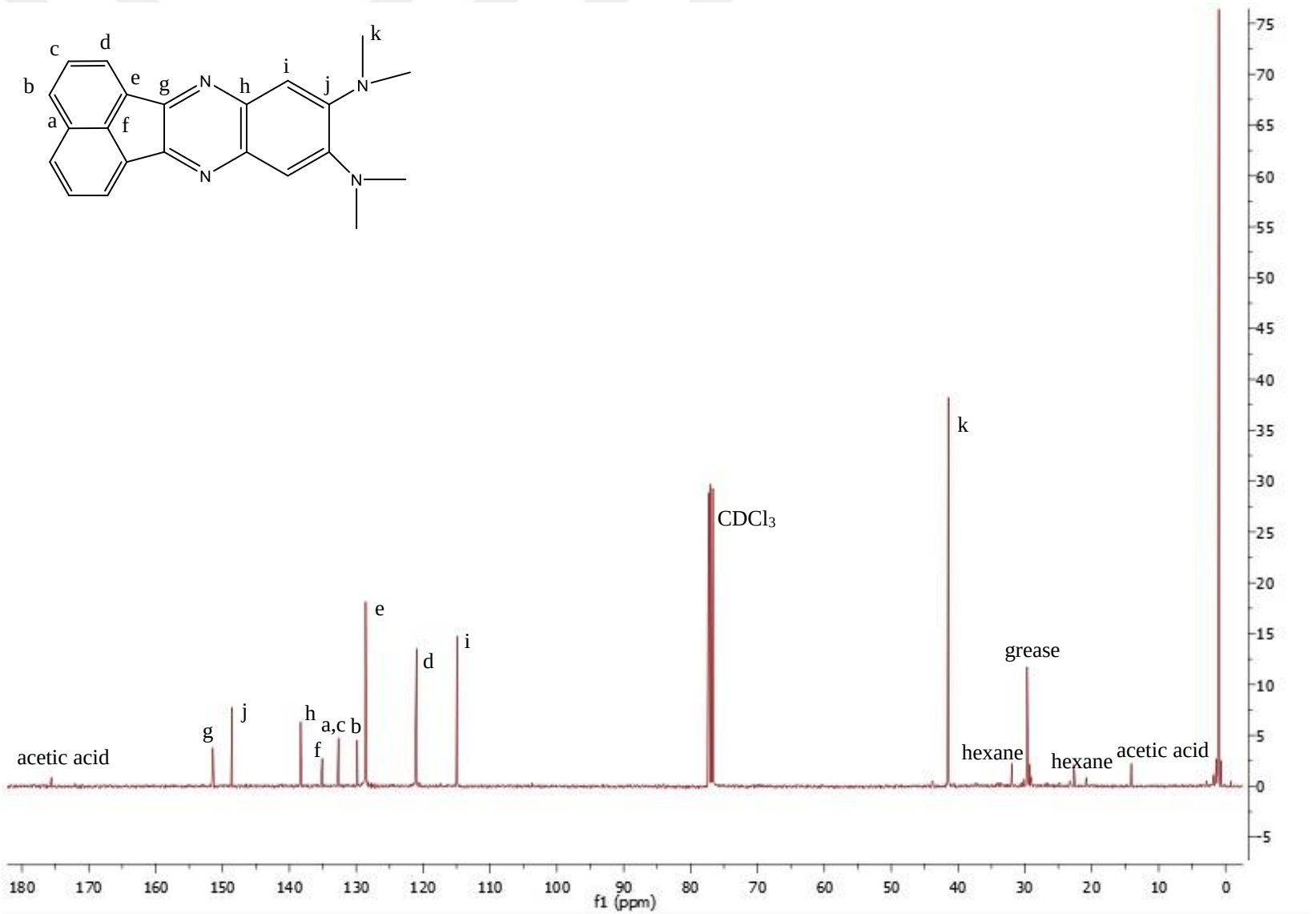


Figure A.6. ^{13}C-NMR Spectrum of N^9, N^9, N^{10}, N^{10}- tetramethylacenaphtho [1, 2-b] quinoxaline-9, 10-diamine in $CDCl_3$.

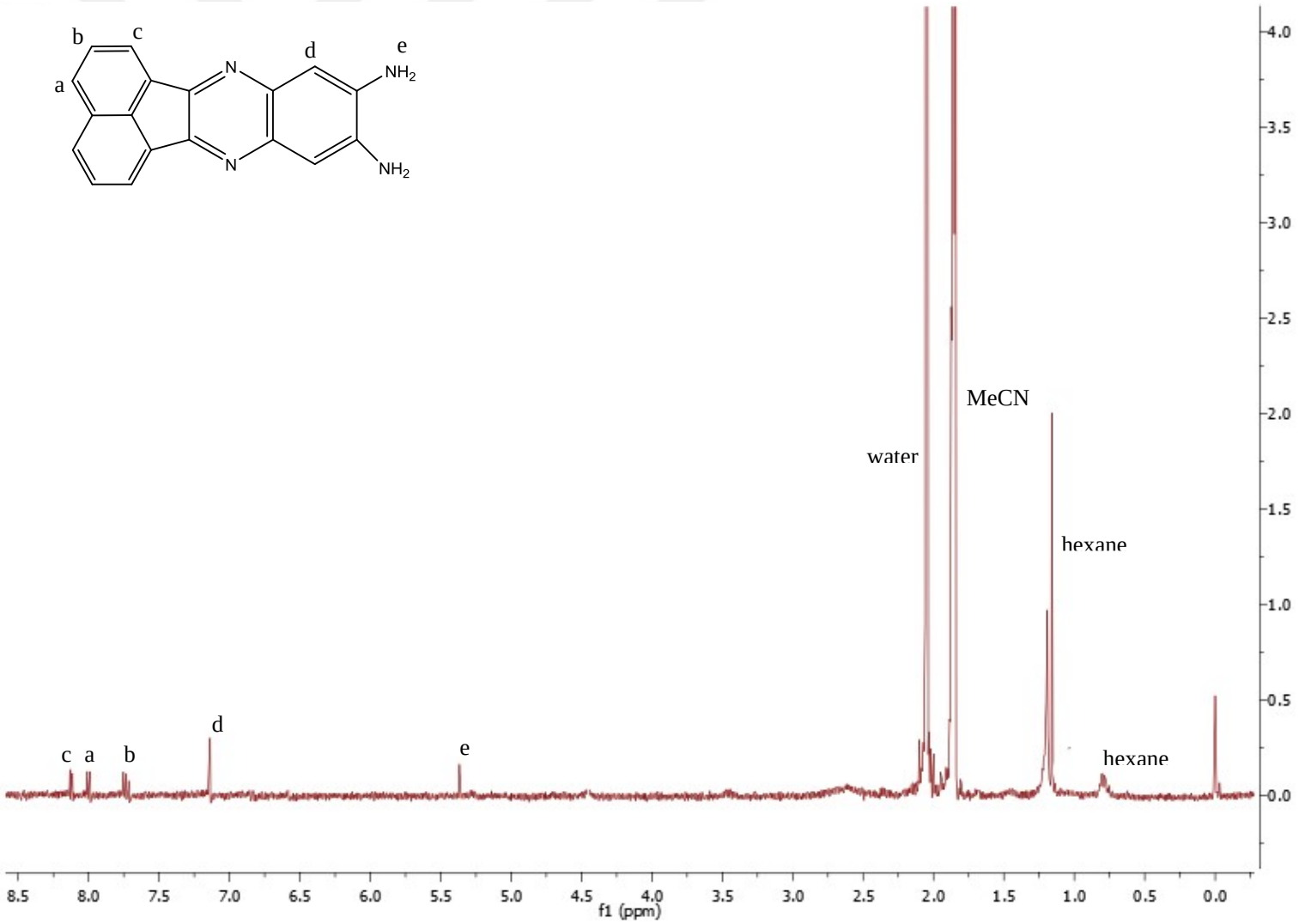


Figure A.7. ^{1}H-NMR Spectrum of Acenaphtho [1, 2-b] quinoxaline-9, 10-diamine in CD_3CN.

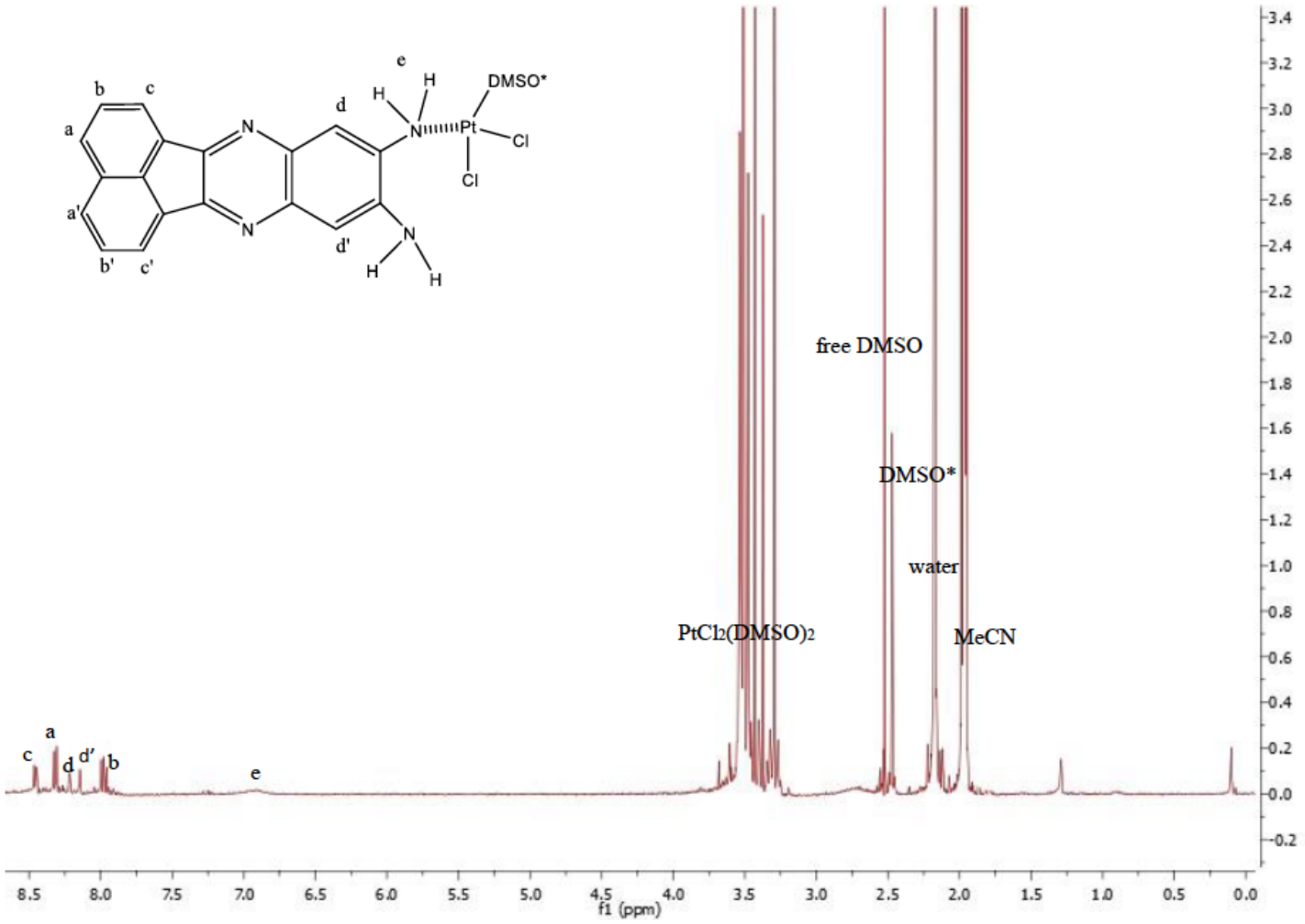


Figure A.8. ^{1}H-NMR Spectrum of Acenaphtho [1, 2-b] quinoxaline-9, 10-diamine Platinum Complex in CD_3CN.